

United Nations Educational, Scientific and Cultural Organization
and
International Atomic Energy Agency

THE ABDUS SALAM INTERNATIONAL CENTRE FOR THEORETICAL PHYSICS

**S-WAVE'S VELOCITIES OF THE LITHOSPHERE-ASTHENOSPHERE
SYSTEM IN THE CARIBBEAN REGION**

O'Leary Gonzalez¹

*Centro Nacional de Investigaciones Sismológicas,
Ministerio de Ciencia, Tecnología y Medio Ambiente, Cuba
and*

The Abdus Salam International Centre for Theoretical Physics, Trieste, Italy,

José Leonardo Alvarez, Bladimir Moreno

*Centro Nacional de Investigaciones Sismológicas,
Ministerio de Ciencia, Tecnología y Medio Ambiente, Cuba*

and

Giuliano F. Panza

*Department of Earth Sciences, University of Trieste, Trieste, Italy
and*

The Abdus Salam International Centre for Theoretical Physics, Trieste, Italy.

MIRAMARE – TRIESTE

June 2010

¹ Regular Associate of ICTP. oleary@sssn.ciges.inf.cu

Abstract

An overview of the S-wave velocity (V_s) structural model of the Caribbean is presented with a resolution of $2^\circ \times 2^\circ$. As a result of the frequency time analysis (FTAN) of more than 400 trajectories epicenter-stations in this region, new tomographic maps of Rayleigh waves group velocity dispersion at periods ranging from 10 s to 40 s have been determined. For each $2^\circ \times 2^\circ$ cell, group velocity dispersion curves were determined and extended to 150 s adding data from a larger scale tomographic study (Vdovin et al., 1999). Using, as independent a priori information, the available geological and geophysical data of the region, each dispersion curve has been mapped, by non-linear inversion, into a set of V_s vs. depth models in the depth range from 0 km to 300 km. Due to the non-uniqueness of the solutions for each cell a Local Smoothness Optimization (LSO) has been applied to the whole region to identify a tridimensional model of V_s vs. depth in cells of $2^\circ \times 2^\circ$, thus satisfying the Occam razor concept. Through these models some main features of the lithosphere and asthenosphere are evidenced, such as: the west directed subduction zone of the eastern Caribbean region with a clear mantle wedge between the Caribbean lithosphere and the subducted slab; the complex and asymmetric behavior of the crustal and lithospheric thickness in the Cayman ridge; the diffused presence of oceanic crust in the region; the presence of continental type crust in the South America, Central America and North America plates, as well as the bottom of the upper asthenosphere that gets shallower going from west to east.

Introduction

The structure of the crust and upper mantle of the Caribbean region, located between the Pacific and Atlantic oceans and the North and South America plates (Figure 1) has been studied by several authors. Regional studies (Dengo and Case, 1990, Van Der Hilst, 1990, Vdovin et al., 1999, Bassin et al., 2000, Chulick and Mooney, 2002, Ligorría and Molina, 1997, Moreno et al. 2002, Pindell and Kennan 2001, Gonzalez et al., 2007, Miller et al., 2009, Growdon et al., 2009, Magnani et al., 2009) and global studies (Laske and Masters, 1997, Montagner and Kennet, 1996, Mooney et al., 1998) clearly evidence the complexity of the region with the presence of continental and accretionary crust, subduction zones, rifts, and predominance of oceanic crust.

The studies of the Caribbean crust and mantle have been made using mainly the available geophysical information and seismic profiles. Few previous studies have used the scarce seismic signals recorded by global, regional broad-band stations and temporary networks for specific local studies. Recently, new broad band stations have been installed in the Caribbean for several reasons, including the need of the tsunami warning system in the region. The United States Geological Survey (USGS) and the Venezuelan Foundation of Seismological Research (FUNVISIS) have installed most of them and in the last months several signals have been recorded, which are very useful for surface waves dispersion analysis in the whole region.

Several, very different models, have been proposed so far to describe the origin and evolution of the Caribbean; some of the most representative models are summarized by Iturralde and Lidiak (2000). Recently Pindell and Kennan (2009) formulate a comprehensive hypotheses about the origin, the evolution of the Caribbean lithosphere and its interaction with American Cordillera, from Baja California to northern Peru, as well as its progressive motion relative to North and South America plates.

The purpose of this paper is to present a three-dimensional Vs. vs depth model of the Caribbean region obtained from Rayleigh wave dispersion analysis and its nonlinear inversion, which is consistent with the available knowledge about the lithosphere-asthenosphere system and provides new information about the regions not studied so far.

Seismic data and processing

From several thousands of waveforms recorded by the stations in the region (Table 1), mainly by USGS and FUNVISIS networks, 206 records (Figure 2) of Rayleigh waves crossing the Caribbean and fulfilling the following conditions about the earthquake source have been selected: depth $h < 75$ km, magnitude $M_s > 5.0$, Latitude (North): $10^\circ - 35^\circ$, Longitude (West): $40^\circ - 140^\circ$. The paths mainly sample the eastern zone of the Caribbean where the spatial resolution of previous studies was the poorest.

Frequency Time Analysis (FTAN) (Levshin et al., 1972), in its most updated version (Levshin et al., 1992), has been used to process the records and the dispersion curves have been determined in the period range from 10 s to 40 s, compatible with the characteristics of the BB stations installed by FUNVISIS, the network with the highest number of stations in the Eastern Caribbean, equipped with Guralp CMG-40T seismometers.

The measurement errors of the group velocity values are consistent with those of a previous study in the region (Gonzalez et al., 2007) and vary from 0.06 km/s to 0.09 km/s.

Using the tomographic procedure described by Ditmar and Yanovskaya (1987), Yanovskaya and Ditmar (1990), Wu and Levshin (1994), and Yanovskaya (1997) new tomographic maps

of the group velocity in the Caribbean were determined for periods from 10 s to 40 s at intervals of 5 s (Figure 3). These maps are an improved and extended version of those obtained by Gonzalez et al. (2007) in the southeast part of the Caribbean.

The lateral resolution, a , shown in Figure 4, is better than 500 km in the whole region, including the southeastern part of the Caribbean and the Lesser Antilles, except for the period of 10 s. The stretching parameter ϵ that indicates the dominant orientation of the paths (Figure 5) indicates a satisfactory uniform spatial distribution of the paths in the study area, where the lateral resolution is better than 500 km.

Non-linear inversion and Local Smoothness Optimization

As a result of the tomographic maps, for each cell of $2^\circ \times 2^\circ$ of the region, a group velocity dispersion curve for periods from 10 s to 40 s (at intervals of 5 s) has been determined (see Appendix 1). These dispersion curves are the input for the non-linear inversion procedure “hedgehog” (Valyus, 1968) used for determining Vs vs. depth models.

The study area has been sampled by Vdovin et al. (1999) with a broader-than-our regional scale tomography, using path lengths longer than 4500 km. The density of these paths is lower, the azimuthal distribution is less uniform than in our study, and the determination of geologically meaningful group velocities for periods less than 30 s is questionable over distances of several thousands of km. On the contrary, the group velocity tomographic results of Vdovin et al. (1999) can be readily used to extend our dispersion relations to longer periods, in the range from 50 s to 150 s, because in this period range the dispersion curves are mainly controlled by deep structural features which are, as a rule, characterized by lateral extensions that are much larger than the shallow ones. To be conservative, as an experimental error associated at each period we consider the same values determined at the shorter periods (ranging from 0.06 km/s to 0.09 km/s) and not the smaller values determined by Vdovin et al. (1999) along much longer profiles.

The values of the parameters describing the sedimentary layers and the upper crust are fixed according to the information available for each cell and where the available information is less detailed or absent, information from global models of the crust (Mooney et al., 1998), sediments (Laske and Masters, 1997) and bathymetry (Smith and Sandwell, 1997) are used.

For layers at depth greater than 350 km for all the cells the models are fixed from already published models, e.g. Montagner and Kennet (1996) and Du et al. (1998).

For each of the 5 inverted layers, the P-wave velocity is determined from the relationship $V_p/V_s = \sqrt{3}$ and, due to its low influence on the final results (e.g. see Panza, 1981), the density is fixed at the beginning of the inversion from the Nafe and Drake relationship (Grant and West, 1965; Fowler, 1995).

The parameterization of the input data and the adequate step ΔP_i for each inverted parameter are defined following the procedure described by Panza (1981) and using the codes developed by Urban et al. (1993) for the analytical determination of the partial derivatives of the dispersion relations with respect to the structural parameters.

The inversion procedure is a Monte Carlo search (to find, in a fully non-linear form, the Vs vs. depth models consistent with the dispersion curves) optimized with the use of a guided method that remembers the results of the previous trials. For each model of the search, which are several thousands, a theoretical dispersion curve is calculated and solutions of the inversion (Biswas and Knopoff, 1974; Panza, 1981) are considered those models for which, at each period, the difference between the theoretical and the experimental values is less than the

measurement error and if the r.m.s. value of the differences, along the entire dispersion curve, is less than the 60% of the average experimental error in the entire period range inverted.

Using this procedure for each cell of $2^{\circ} \times 2^{\circ}$, a set of models which are solutions of the inversion according to all the available geophysical and geological information, is determined and their number for each cell varies from 10 to 30 models.

Several criteria have been applied for the selection of one model for each cell from the set of solutions (Shapiro and Ritzwoller, 2002; Gonzalez et al., 2007). Considering that all the models are consistent with the geological and geophysical information, some optimization methods to select a model for each cell are described by Boyadzhiev et al. (2008). These methods are based on the concept of William of Occam razor “it is vain to do with more what can be done with less”.

In our case, we choose the Local Smoothness Optimization method (LSO) (Boyadzhiev et al., 2008) not only because it is very fast, but because it is quite appropriate for a region with very large heterogeneities (like the Caribbean).

As a final result, the model of Vs up to 300 km of depth in 85 ($2^{\circ} \times 2^{\circ}$) cells is obtained (see Figures 6-8 and Appendix 2), representing the first approximation, at this level of detail, of the structure of the lithosphere-asthenosphere system in the Caribbean region.

Results and discussion

The tomographic maps cover the southeastern part of the Caribbean and its subduction zone and extend the area coverage of the previous study by Gonzalez et al. (2007).

At the southeast end of the study area, a relatively low group velocity in the period range from 20 s to 40 s is found (Figure 3), consistent with the presence of the subduction zone and of the older part of the Caribbean crust (Pindell and Kennan, 2009). In the southern part, at some periods, the group velocity is as low as in the northern part of the South America plate where the crust is mainly continental (Dengo and Case, 1990, Pindell and Kennan, 2001). Such a situation could be explained by the known contact between the accretionary wedge (the Barbados prism), the right-lateral transpression and clockwise rotations of the thrust sheets in the southern part of a West-directed subduction zone (Doglioni et al., 1999).

The Vs structure of the Caribbean is shown in Figures 6, 7 and 8 up to 50 km, 150 km and 300 km of depth, respectively. In the uppermost 50 km (Figure 6), in the northern part of South America Plate and the South Caribbean fold belt (cells in 74° - 62° W, 10° N) it is evident the predominant presence of continental crust ~30 km thick (Dengo and Case, 1990), while in the northeastern most part of the region (cells in 60° W, 16° - 18° N) a typically oceanic crust is present, which could belong to the younger Atlantic crust.

Well defined thick crusts, in some known typical continental crust areas like in the northeast of Yucatan (cells in 86° W, 22° N), Central America coinciding with the Chortis blocks (cell in 84° W, 14° N) (Dengo and Case, 1990), and the western of Cuba (cells in 82° W, 20° - 22° N) (Tenreyro et. al., 1994) are evidenced. To the east of the Chortis block (cells in 82° - 74° W, 14° N; 74° - 70° W, 16° N and 70° W, 18° N) mostly coinciding with the Hess Escarpment (Pindell and Kennan, 2009), relatively high velocities values in the upper crust are found.

Figure 6 evidences other main features of the Caribbean crust like the Mid-Cayman spreading center (MCSC) (cell in 86° - 82° W, 18° N) with very thin sedimentary layers overlaying the uppermost lithospheric mantle. Along the profile A-A' of Figure 9, mostly coinciding with the MCSC and the Cayman trough, in good agreement with previous studies by Ten Brink et al. (2001), the thinnest crust is seen to the west of the ridge, while to the east

the crust is accreted by new material rising from the ridge. A relatively shallower basement in the easternmost part of Cayman trough (cells in 80°-78°W, 18°N, see also Figure 6) is also consistent with previous results from modeling of the gravity field (Ten Brink et al., 2002). The lithosphere is thicker in the west side of the MCSC than in the east side which is in good agreement with the global asymmetric pattern of the deep part of ridges evidenced by Panza et al. (2010).

In coincidence with the region where the Atlantic plate is subducted under the Caribbean Plate (Pindell and Kennan, 2009) (cells 64°W, 18°N; 62°W, from 10° to 18°N and 60°W, from 12° to 18°N and profile B-B' of Figure 9), low velocities characterize the upper mantle and mark the presence of the mantle wedge included between the upper and lower plate of the west directed subduction process (Doglioni et al., 2009).

Crustal thickness in the western part of the Caribbean plate (cells in 80°-70°W, 12°-18°N in Figure 6) ranges from 20km to 25 km while to the east (cells in 68°-62°W, 14°-16°N) the crust is thinner and some low velocity values are present in the upper mantle (see also profile B-B' of Figure 9). Such feature is well consistent with presence of the wide back arc basin (Pindell and Kennan, 2001) and the rejuvenation from west to east of the Caribbean plate due to the eastward retreat of the subduction zone (Doglioni et al., 2007).

The lithospheric thicknesses are well defined in the major strike-slip fault zones and the velocities for the deepest lithospheric layers are, in general, relatively high. In the southernmost part (cells from 74° to 62°W, 10°N), i.e. in the South America Plate and the South Caribbean fold belt, the lithosphere thickness varies between 80 km and 120 km and to the northwestern side of such faults system the underthrusting of the South America plate by the Caribbean slab (the so-called Caribbean Large Igneous Province CLIP (Miller et al., 2009)), is evident (in cells 72°W, 14°N and 70°W, from 12° to 14°N) as can be seen in Figures 6, 7 and profile B-B' of figure 9.

At the boundary between the North America Plate and the Caribbean Plate (cells 82°W, 18°N and from 80°W to 70°W, 20°N) the lithospheric thickness has a significant increase at the contact between the Gonave Microplate and Hispaniola Island (in cells from 76°W to 74°W, 20°N). This lithospheric thickening from 80 km to more than 130 km is related to the presence of several major active tectonic structures on Hispaniola Island, which accommodate the relative motion between the Caribbean, the North America Plate and the Gonave Microplate (Mann et al., 1998, 2002; Pindell and Kennan, 2009).

In the Caribbean, the bottom of the upper asthenosphere, within which sometimes a well developed low velocity zone is present, gets shallower going from west to east, from around 250 km in the east of Central America to about 160 km in the Lesser Antilles (Figure 8).

Conclusions

The three-dimensional Vs. vs depth model of the Caribbean region obtained is consistent with the available knowledge about the lithosphere-asthenosphere system, and provides new information about the regions not studied so far.

The 1-D models of Vs vs. depth determined by non-linear inversion for 2° x 2° cells are processed with a Local Smoothness Optimization procedure and supply a 3-D structure, with its uncertainties, of the Caribbean down to a depth of about 300 km, with unprecedented detail. In this model some important features of the structure of the Caribbean crust are well distinguished, like the diffused presence of oceanic crust in the region, the thick continental crust in the South America plate and others isolated regions in Central America, as well as the rejuvenation from west to east of the crust in the Caribbean Plate. In the major strike-slips

fault zones (between the North America plate, South America plate and the Caribbean Plate) the lithospheric thickness ranges from 80 km to 130 km and, in such zones, the velocity values in the lower lithosphere are relatively high. The crust and lithosphere thickness to the west and east of the Middle Cayman Spreading Center are asymmetric, the crust is thinner to the west while the lithosphere is thicker. To the east of the MCSC the new mantle material accreted the existing crust while from more than 200 km east of the rise the crust becomes thinner. Several cells, mainly belonging to the Hess Escarpment, have high velocity layers in the upper crust while more to the east the underthrusting of the South America plate by the Caribbean Plate is well visible. In the Caribbean Plate, going from west to east, the top of the lower asthenosphere gets shallower from around 250 km, in the east of Central America, to about 160 km in the subduction zone.

Acknowledgments

The authors express thanks to Anatoli L. Levshin from the University of Colorado, for kindly providing us with the long-period group velocities available at CIEI, University of Colorado at Boulder and the staff of the Earth Science Department of the University of Trieste for all their help and facilities, especially to Enrico Brandmayr for the use of the LSO code. The authors also want to express their thanks to Julio Garcia, from National Institute of Oceanography, Geophysics and Seismology (OGS) of Italy and to Carlo Doglioni for their help in the geological interpretation of results. The present work is done with the financial support of the Associate Scheme, TRIL Programs and ESP (SAND group) Section of the “Abdus Salam” International Centre for Theoretical Physics, the Ministry of Science, Technology and Environment of Cuba through projects PNCB 020/04, PTCT 17-05 and PTSCu 08-8, as well as founded by the Italian MIUR Cofin-2001 (2001045878_007), Cofin-2002 (2002047575_002), the Italian Programma Nazionale di Ricerche in Antartide (PNRA) 2004-2006, project 2.7–2.8 (“Sismologia a larga banda nella regione del Mare di Scotia e suo utilizzo per lo studio della geodinamica della litosfera”) and the UNESCO through Project UNESCO/IGCP 487 and from ICTP through Network NET-58.

Appendix 1. Values of group velocity dispersion curves for each cell.

| Period T(s) | Group velocity (km/s) | | | | | | | | | | | | |
|----------------|-----------------------|-----------------|-----------------|-----------------|-----------------|-----------------|-----------------|-----------------|-----------------|-----------------|-----------------|-----------------|-----------------|
| | W-62.0 N10.0 | W-64.0 N10.0 | W-66.0 N10.0 | W-68.0 N10.0 | W-70.0 N10.0 | W-72.0 N10.0 | W-74.0 N10.0 | W-76.0 N10.0 | W-78.0 N10.0 | W-80.0 N10.0 | W-82.0 N10.0 | W-84.0 N10.0 | W-60.0 N12.0 |
| 10 | | | | | | | 2.278 | 2.300 | 2.287 | 2.469 | 2.350 | 2.069 | |
| 15 | | | 2.739 | 2.792 | 2.619 | 2.606 | 2.620 | 2.558 | 2.507 | 2.749 | 2.742 | 2.596 | 2.630 |
| 20 | 2.571 | 2.678 | 2.729 | 2.716 | 2.633 | 2.559 | 2.622 | 2.758 | 3.015 | 3.103 | 3.051 | 3.017 | 2.620 |
| 25 | 2.783 | 2.897 | 3.013 | 2.949 | 2.864 | 2.803 | 2.855 | 2.946 | 3.271 | 3.459 | 3.478 | 3.308 | 2.793 |
| 30 | 3.116 | 3.199 | 3.312 | 3.289 | 3.203 | 3.148 | 3.121 | 3.146 | 3.407 | 3.583 | 3.715 | 3.630 | 3.199 |
| 35 | 3.272 | 3.361 | 3.501 | 3.459 | 3.395 | 3.326 | 3.299 | 3.305 | 3.505 | 3.694 | 3.786 | 3.663 | 3.392 |
| 40 | 3.388 | 3.453 | 3.549 | 3.567 | 3.541 | 3.488 | 3.432 | 3.440 | 3.626 | 3.741 | 3.827 | 3.667 | 3.509 |
| 60 | 3.817 | 3.842 | 3.856 | 3.856 | 3.841 | 3.823 | 3.809 | 3.796 | 3.801 | 3.798 | 3.785 | 3.784 | 3.745 |
| 80 | 3.802 | 3.832 | 3.855 | 3.868 | 3.868 | 3.862 | 3.851 | 3.835 | 3.828 | 3.814 | 3.793 | 3.795 | 3.730 |
| 100 | 3.808 | 3.836 | 3.857 | 3.870 | 3.873 | 3.864 | 3.842 | 3.817 | 3.799 | 3.782 | 3.771 | 3.770 | 3.736 |
| 125 | 3.843 | 3.838 | 3.833 | 3.828 | 3.824 | 3.812 | 3.795 | 3.779 | 3.757 | 3.730 | 3.710 | 3.703 | 3.836 |
| 150 | 3.789 | 3.792 | 3.793 | 3.790 | 3.785 | 3.778 | 3.768 | 3.755 | 3.738 | 3.721 | 3.707 | 3.709 | 3.777 |

| Period T(s) | Group velocity (km/s) | | | | | | | | | | | | |
|----------------|-----------------------|-----------------|-----------------|-----------------|-----------------|-----------------|-----------------|-----------------|-----------------|-----------------|-----------------|-----------------|-----------------|
| | W-62.0 N12.0 | W-64.0 N12.0 | W-66.0 N12.0 | W-68.0 N12.0 | W-70.0 N12.0 | W-72.0 N12.0 | W-74.0 N12.0 | W-76.0 N12.0 | W-78.0 N12.0 | W-80.0 N12.0 | W-82.0 N12.0 | W-84.0 N12.0 | W-60.0 N14.0 |
| 10 | | | | | | | 2.273 | 2.303 | 2.286 | 2.550 | 2.433 | 2.176 | |
| 15 | 2.513 | 2.511 | 2.579 | 2.547 | 2.475 | 2.438 | 2.472 | 2.487 | 2.456 | 2.638 | 2.649 | 2.569 | 2.654 |
| 20 | 2.567 | 2.745 | 2.949 | 2.979 | 2.893 | 2.789 | 2.869 | 3.008 | 3.314 | 3.359 | 3.229 | 3.045 | 2.820 |
| 25 | 2.898 | 3.061 | 3.209 | 3.176 | 3.090 | 3.087 | 3.190 | 3.228 | 3.469 | 3.572 | 3.485 | 3.295 | 3.001 |
| 30 | 3.156 | 3.293 | 3.455 | 3.398 | 3.300 | 3.311 | 3.378 | 3.392 | 3.577 | 3.673 | 3.692 | 3.554 | 3.317 |
| 35 | 3.312 | 3.418 | 3.577 | 3.549 | 3.482 | 3.492 | 3.511 | 3.513 | 3.647 | 3.744 | 3.743 | 3.609 | 3.476 |
| 40 | 3.421 | 3.486 | 3.585 | 3.648 | 3.648 | 3.645 | 3.637 | 3.623 | 3.745 | 3.814 | 3.796 | 3.654 | 3.622 |
| 60 | 3.781 | 3.813 | 3.838 | 3.849 | 3.847 | 3.851 | 3.852 | 3.848 | 3.829 | 3.811 | 3.789 | 3.778 | 3.715 |
| 80 | 3.758 | 3.782 | 3.812 | 3.833 | 3.846 | 3.859 | 3.865 | 3.862 | 3.851 | 3.840 | 3.823 | 3.800 | 3.700 |
| 100 | 3.766 | 3.793 | 3.818 | 3.836 | 3.845 | 3.846 | 3.838 | 3.825 | 3.807 | 3.791 | 3.777 | 3.766 | 3.704 |
| 125 | 3.833 | 3.827 | 3.819 | 3.815 | 3.809 | 3.792 | 3.776 | 3.761 | 3.751 | 3.735 | 3.712 | 3.690 | 3.824 |
| 150 | 3.771 | 3.765 | 3.765 | 3.767 | 3.769 | 3.765 | 3.759 | 3.754 | 3.745 | 3.732 | 3.718 | 3.710 | 3.781 |

| Period T(s) | Group velocity (km/s) | | | | | | | | | | | | |
|----------------|-----------------------|-----------------|-----------------|-----------------|-----------------|-----------------|-----------------|-----------------|-----------------|-----------------|-----------------|-----------------|-----------------|
| | W-62.0 N14.0 | W-64.0 N14.0 | W-66.0 N14.0 | W-68.0 N14.0 | W-70.0 N14.0 | W-72.0 N14.0 | W-74.0 N14.0 | W-76.0 N14.0 | W-78.0 N14.0 | W-80.0 N14.0 | W-82.0 N14.0 | W-84.0 N14.0 | W-60.0 N16.0 |
| 10 | | | | | | 2.298 | 2.270 | 2.236 | 2.148 | 2.443 | 2.741 | 2.565 | |
| 15 | 2.524 | 2.543 | 2.525 | 2.406 | 2.434 | 2.432 | 2.418 | 2.398 | 2.290 | 2.546 | 2.767 | 2.875 | 2.721 |
| 20 | 2.961 | 3.021 | 3.067 | 3.118 | 3.225 | 3.281 | 3.261 | 3.233 | 3.395 | 3.309 | 3.224 | 3.093 | 3.013 |
| 25 | 3.210 | 3.342 | 3.388 | 3.343 | 3.451 | 3.629 | 3.617 | 3.481 | 3.679 | 3.598 | 3.443 | 3.323 | 3.239 |
| 30 | 3.389 | 3.489 | 3.583 | 3.563 | 3.653 | 3.754 | 3.706 | 3.625 | 3.706 | 3.709 | 3.629 | 3.494 | 3.443 |
| 35 | 3.527 | 3.587 | 3.703 | 3.716 | 3.784 | 3.840 | 3.810 | 3.752 | 3.795 | 3.785 | 3.712 | 3.592 | 3.541 |
| 40 | 3.644 | 3.631 | 3.699 | 3.802 | 3.891 | 3.917 | 3.888 | 3.815 | 3.866 | 3.872 | 3.745 | 3.642 | 3.691 |
| 60 | 3.757 | 3.790 | 3.821 | 3.844 | 3.866 | 3.883 | 3.883 | 3.869 | 3.854 | 3.840 | 3.832 | 3.808 | 3.690 |
| 80 | 3.736 | 3.761 | 3.784 | 3.806 | 3.833 | 3.855 | 3.865 | 3.867 | 3.861 | 3.855 | 3.852 | 3.838 | 3.679 |
| 100 | 3.739 | 3.768 | 3.789 | 3.808 | 3.822 | 3.830 | 3.831 | 3.825 | 3.811 | 3.800 | 3.790 | 3.783 | 3.679 |
| 125 | 3.815 | 3.807 | 3.803 | 3.795 | 3.784 | 3.776 | 3.761 | 3.755 | 3.750 | 3.741 | 3.721 | 3.698 | 3.808 |
| 150 | 3.776 | 3.772 | 3.766 | 3.761 | 3.754 | 3.750 | 3.750 | 3.748 | 3.745 | 3.736 | 3.722 | 3.703 | 3.775 |

| Period T(s) | Group velocity (km/s) | | | | | | | | | | | | |
|----------------|-----------------------|-----------------|-----------------|-----------------|-----------------|-----------------|-----------------|-----------------|-----------------|-----------------|-----------------|-----------------|-----------------|
| | W-62.0 N16.0 | W-64.0 N16.0 | W-66.0 N16.0 | W-68.0 N16.0 | W-70.0 N16.0 | W-72.0 N16.0 | W-74.0 N16.0 | W-76.0 N16.0 | W-78.0 N16.0 | W-80.0 N16.0 | W-82.0 N16.0 | W-84.0 N16.0 | W-86.0 N16.0 |
| 10 | | | | 2.258 | 2.307 | 2.333 | 2.394 | 2.321 | 2.232 | 2.631 | 2.867 | 2.848 | 2.520 |
| 15 | 2.619 | 2.612 | 2.470 | 2.392 | 2.484 | 2.423 | 2.387 | 2.433 | 2.481 | 2.822 | 2.964 | 3.091 | 2.822 |
| 20 | 3.063 | 3.169 | 3.179 | 3.263 | 3.399 | 3.325 | 3.185 | 3.065 | 3.130 | 3.184 | 3.230 | 3.414 | 3.225 |
| 25 | 3.319 | 3.443 | 3.484 | 3.609 | 3.763 | 3.652 | 3.480 | 3.328 | 3.447 | 3.440 | 3.488 | 3.622 | 3.460 |
| 30 | 3.467 | 3.592 | 3.675 | 3.801 | 3.878 | 3.791 | 3.666 | 3.565 | 3.587 | 3.576 | 3.609 | 3.627 | 3.599 |
| 35 | 3.555 | 3.664 | 3.745 | 3.869 | 3.937 | 3.872 | 3.767 | 3.730 | 3.732 | 3.672 | 3.652 | 3.618 | 3.659 |
| 40 | 3.671 | 3.688 | 3.747 | 3.925 | 3.976 | 3.924 | 3.832 | 3.808 | 3.821 | 3.744 | 3.670 | 3.629 | 3.655 |
| 60 | 3.737 | 3.778 | 3.812 | 3.845 | 3.884 | 3.898 | 3.897 | 3.888 | 3.875 | 3.863 | 3.857 | 3.849 | 3.823 |
| 80 | 3.723 | 3.756 | 3.781 | 3.802 | 3.823 | 3.845 | 3.858 | 3.867 | 3.870 | 3.868 | 3.869 | 3.865 | 3.847 |
| 100 | 3.720 | 3.752 | 3.777 | 3.796 | 3.810 | 3.824 | 3.830 | 3.829 | 3.822 | 3.810 | 3.805 | 3.796 | 3.786 |
| 125 | 3.797 | 3.793 | 3.783 | 3.775 | 3.769 | 3.758 | 3.755 | 3.748 | 3.741 | 3.731 | 3.720 | 3.708 | 3.707 |
| 150 | 3.779 | 3.780 | 3.779 | 3.774 | 3.769 | 3.765 | 3.759 | 3.751 | 3.742 | 3.727 | 3.711 | 3.692 | 3.683 |

| Period T(s) | Group velocity (km/s) | | | | | | | | | | | | |
|----------------|-----------------------|-----------------|-----------------|-----------------|-----------------|-----------------|-----------------|-----------------|-----------------|-----------------|-----------------|-----------------|-----------------|
| | W-60.0 N18.0 | W-62.0 N18.0 | W-64.0 N18.0 | W-66.0 N18.0 | W-68.0 N18.0 | W-70.0 N18.0 | W-72.0 N18.0 | W-74.0 N18.0 | W-76.0 N18.0 | W-78.0 N18.0 | W-80.0 N18.0 | W-82.0 N18.0 | W-84.0 N18.0 |
| 10 | | | 2.514 | 2.499 | 2.493 | 2.541 | 2.586 | 2.634 | 2.511 | 2.315 | 2.584 | 2.759 | 2.873 |
| 15 | 2.782 | 2.730 | 2.658 | 2.446 | 2.404 | 2.563 | 2.622 | 2.639 | 2.534 | 2.508 | 2.807 | 3.038 | 3.224 |
| 20 | 3.176 | 3.102 | 3.013 | 2.975 | 2.908 | 2.976 | 3.051 | 3.104 | 3.068 | 3.124 | 3.282 | 3.413 | 3.579 |
| 25 | 3.423 | 3.452 | 3.326 | 3.241 | 3.235 | 3.293 | 3.338 | 3.364 | 3.383 | 3.428 | 3.555 | 3.674 | 3.731 |
| 30 | 3.600 | 3.611 | 3.508 | 3.433 | 3.450 | 3.470 | 3.520 | 3.571 | 3.594 | 3.603 | 3.670 | 3.785 | 3.731 |
| 35 | 3.696 | 3.702 | 3.628 | 3.547 | 3.543 | 3.566 | 3.608 | 3.657 | 3.720 | 3.744 | 3.745 | 3.772 | 3.728 |
| 40 | 3.788 | 3.772 | 3.708 | 3.661 | 3.626 | 3.652 | 3.657 | 3.690 | 3.758 | 3.808 | 3.812 | 3.762 | 3.746 |
| 60 | 3.660 | 3.714 | 3.761 | 3.807 | 3.849 | 3.874 | 3.891 | 3.902 | 3.903 | 3.895 | 3.883 | 3.876 | 3.868 |
| 80 | 3.649 | 3.706 | 3.747 | 3.782 | 3.810 | 3.828 | 3.841 | 3.853 | 3.867 | 3.878 | 3.883 | 3.885 | 3.884 |
| 100 | 3.648 | 3.699 | 3.738 | 3.769 | 3.795 | 3.815 | 3.826 | 3.834 | 3.838 | 3.837 | 3.831 | 3.824 | 3.816 |
| 125 | 3.802 | 3.790 | 3.774 | 3.765 | 3.755 | 3.747 | 3.744 | 3.741 | 3.735 | 3.735 | 3.742 | 3.740 | 3.733 |
| 150 | 3.779 | 3.772 | 3.776 | 3.780 | 3.785 | 3.788 | 3.790 | 3.786 | 3.778 | 3.763 | 3.745 | 3.725 | 3.701 |

| Period T(s) | Group velocity (km/s) | | | | | | | | | | | | |
|----------------|-----------------------|-----------------|-----------------|-----------------|-----------------|-----------------|-----------------|-----------------|-----------------|-----------------|-----------------|-----------------|-----------------|
| | W-86.0 N18.0 | W-70.0 N20.0 | W-72.0 N20.0 | W-74.0 N20.0 | W-76.0 N20.0 | W-78.0 N20.0 | W-80.0 N20.0 | W-82.0 N20.0 | W-84.0 N20.0 | W-86.0 N20.0 | W-82.0 N22.0 | W-84.0 N22.0 | W-86.0 N22.0 |
| 10 | 2.729 | 2.611 | 2.527 | 2.486 | 2.424 | 2.376 | 2.543 | 2.561 | 2.778 | 2.677 | 2.487 | 2.457 | 2.558 |
| 15 | 3.167 | 2.631 | 2.598 | 2.576 | 2.594 | 2.688 | 2.832 | 3.021 | 3.018 | 2.808 | 2.731 | 2.658 | 2.769 |
| 20 | 3.478 | 2.829 | 2.779 | 2.837 | 2.953 | 3.100 | 3.088 | 3.103 | 3.153 | 3.055 | 2.955 | 2.968 | 2.995 |
| 25 | 3.628 | 3.042 | 3.040 | 3.122 | 3.320 | 3.382 | 3.361 | 3.460 | 3.547 | 3.421 | 3.239 | 3.292 | 3.214 |
| 30 | 3.645 | 3.322 | 3.298 | 3.381 | 3.551 | 3.548 | 3.515 | 3.653 | 3.664 | 3.556 | 3.554 | 3.554 | 3.416 |
| 35 | 3.697 | 3.444 | 3.419 | 3.524 | 3.702 | 3.718 | 3.629 | 3.673 | 3.702 | 3.623 | 3.633 | 3.661 | 3.532 |
| 40 | 3.726 | 3.576 | 3.546 | 3.623 | 3.769 | 3.825 | 3.672 | 3.664 | 3.719 | 3.673 | 3.674 | 3.730 | 3.634 |
| 60 | 3.859 | 3.856 | 3.875 | 3.885 | 3.894 | 3.899 | 3.895 | 3.887 | 3.878 | 3.869 | 3.894 | 3.885 | 3.875 |
| 80 | 3.876 | 3.824 | 3.839 | 3.847 | 3.855 | 3.876 | 3.887 | 3.895 | 3.897 | 3.891 | 3.891 | 3.894 | 3.891 |
| 100 | 3.803 | 3.812 | 3.829 | 3.838 | 3.842 | 3.852 | 3.853 | 3.852 | 3.845 | 3.829 | 3.863 | 3.855 | 3.842 |
| 125 | 3.738 | 3.757 | 3.759 | 3.762 | 3.768 | 3.773 | 3.779 | 3.782 | 3.782 | 3.769 | 3.824 | 3.810 | 3.797 |
| 150 | 3.683 | 3.799 | 3.801 | 3.795 | 3.786 | 3.775 | 3.765 | 3.753 | 3.735 | 3.716 | 3.768 | 3.754 | 3.737 |

| Period T(s) | Group velocity (km/s) | | | | | | |
|----------------|-----------------------|-----------------|-----------------|-----------------|----------------|----------------|----------------|
| | W-82.0 N24.0 | W-84.0 N24.0 | W-82.0 N26.0 | W-84.0 N26.0 | W-76.0 N8.0 | W-80.0 N8.0 | W-82.0 N8.0 |
| 10 | 2.562 | 2.553 | 2.683 | 2.702 | 2.252 | 2.343 | 2.315 |
| 15 | 2.669 | 2.705 | 2.674 | 2.750 | 2.507 | 2.634 | 2.653 |
| 20 | 2.904 | 2.918 | 2.913 | 2.942 | 2.806 | 3.158 | 3.130 |
| 25 | 3.117 | 3.130 | 3.122 | 3.037 | 2.949 | 3.437 | 3.461 |
| 30 | 3.431 | 3.406 | 3.411 | 3.334 | 3.106 | 3.601 | 3.693 |
| 35 | 3.627 | 3.593 | 3.625 | 3.590 | 3.253 | 3.683 | 3.756 |
| 40 | 3.673 | 3.655 | 3.695 | 3.653 | 3.395 | 3.710 | 3.742 |
| 60 | 3.891 | 3.892 | 3.894 | 3.891 | 3.783 | 3.792 | 3.790 |
| 80 | 3.883 | 3.890 | 3.893 | 3.889 | 3.817 | 3.800 | 3.789 |
| 100 | 3.868 | 3.867 | 3.880 | 3.874 | 3.826 | 3.795 | 3.784 |
| 125 | 3.850 | 3.844 | 3.870 | 3.859 | 3.793 | 3.737 | 3.721 |
| 150 | 3.772 | 3.760 | 3.768 | 3.762 | 3.760 | 3.716 | 3.707 |

Appendix 2. The solution chosen for each cell by LSO from the nonlinear inversion is presented for each cell as layer thickness (km) vs. Vs (km/s). For the first 4 layers the values are fixed from a priori information. The lower 5 layers represent the chosen solution as the range of variability of the parameterized thickness and shear-wave velocity. Frequently the chosen value does not necessarily fall in the center of the variability range that can turn out to be smaller than the step ΔP_i , used in the inversion.

| W-62N10 | | W-64N10 | | W-66N10 | | W-68N10 | | W-70N10 | |
|------------|-----------|------------|-----------|------------|-----------|------------|-----------|------------|-----------|
| h (km) | Vs(km/s) |
| 0.3 | 0.00 | 0.1 | 0.00 | 0.2 | 0.00 | 0.1 | 1.20 | 0.5 | 1.10 |
| 0.5 | 1.20 | 0.5 | 1.20 | 0.1 | 1.23 | 0.6 | 2.10 | 0.5 | 2.10 |
| 3.2 | 2.20 | 2.0 | 2.20 | 1.0 | 1.98 | 2.0 | 3.88 | 6.0 | 3.40 |
| 2.7 | 2.20 | 2.0 | 2.20 | 1.9 | 1.98 | 2.0 | 3.88 | 6.0 | 3.40 |
| 18.0- 22.0 | 3.53-3.63 | 3.5- 5.5 | 2.56-2.76 | 2.0- 4.0 | 2.93-3.13 | 20.0- 24.0 | 3.25-3.40 | 7.5- 12.5 | 3.10-3.30 |
| 10.5- 15.5 | 3.97-4.17 | 17.0- 27.0 | 3.59-3.79 | 21.5- 26.5 | 3.55-3.75 | 6.0- 11.0 | 3.88-4.05 | 7.0- 10.0 | 3.38-3.62 |
| 29.0- 34.0 | 4.45-4.55 | 25.0- 30.0 | 4.40-4.60 | 20.0- 40.0 | 4.40-4.60 | 42.0- 52.0 | 4.40-4.60 | 40.0- 50.0 | 4.38-4.62 |
| 30.0- 70.0 | 4.65-4.75 | 30.0- 70.0 | 4.65-4.75 | 20.0- 42.5 | 4.65-4.70 | 20.0- 40.0 | 4.60-4.70 | 30.0- 55.0 | 4.60-4.80 |
| 55.0-105.0 | 4.40-4.60 | 105-130 | 4.40-4.60 | 110-140 | 4.40-4.60 | 90.0-110.0 | 4.40-4.60 | 80.0-110.0 | 4.40-4.60 |

| W-72N10 | | W-74N10 | | W-76N10 | | W-78N10 | | W-80N10 | |
|------------|-----------|------------|-----------|------------|-----------|------------|-----------|------------|-----------|
| h (km) | Vs(km/s) |
| 1.0 | 1.20 | 0.9 | 1.09 | 1.0 | 0.00 | 0.5 | 0.00 | 1.8 | 0.00 |
| 4.0 | 2.20 | 1.5 | 2.18 | 0.5 | 1.00 | 0.1 | 1.90 | 1.4 | 0.90 |
| 5.0 | 3.50 | 2.0 | 3.50 | 1.3 | 2.00 | 0.1 | 1.93 | 1.2 | 1.80 |
| 6.0 | 3.50 | 2.0 | 3.50 | 1.3 | 2.10 | 0.1 | 2.00 | 1.6 | 1.80 |
| 6.0- 10.0 | 3.50-3.70 | 4.0- 5.5 | 2.50-2.70 | 5.6- 7.6 | 3.15-3.25 | 14.0- 16.0 | 2.95-3.05 | 11.0- 15.0 | 3.70-3.90 |
| 5.0- 7.5 | 3.20-3.35 | 13.8- 21.2 | 3.70-3.90 | 8.0- 12.0 | 3.40-3.50 | 4.5- 6.0 | 3.95-4.25 | 5.0- 8.8 | 3.80-4.00 |
| 40.0- 50.0 | 4.40-4.60 | 32.5- 47.5 | 4.20-4.40 | 40.0- 50.0 | 4.20-4.40 | 7.5- 12.5 | 4.60-4.70 | 20.0- 40.0 | 4.60-4.80 |
| 30.0- 50.0 | 4.62-4.75 | 40.0- 60.0 | 4.60-4.70 | 10.0- 20.0 | 4.60-4.70 | 27.5- 42.5 | 4.20-4.40 | 25.0- 37.5 | 4.20-4.40 |
| 100-120 | 4.40-4.60 | 100-140 | 4.40-4.60 | 130-160 | 4.40-4.60 | 140-160 | 4.40-4.60 | 140-160 | 4.40-4.60 |

| W-82N10 | | W-84N10 | | W-60N12 | | W-62N12 | | W-64N12 | |
|------------|-----------|------------|-----------|------------|-----------|------------|-----------|------------|-----------|
| h (km) | Vs(km/s) |
| 1.8 | 0.00 | 1.0 | 1.10 | 1.8 | 0.00 | 0.4 | 0.00 | 1.4 | 0.00 |
| 1.0 | 1.10 | 3.5 | 2.60 | 2.0 | 1.53 | 6.0 | 2.56 | 1.5 | 2.05 |
| 4.0 | 3.30 | 4.0 | 2.60 | 4.0 | 2.16 | 2.0 | 3.07 | 1.3 | 2.50 |
| 4.2 | 3.30 | 4.5 | 3.50 | 7.0 | 3.39 | 14.0 | 3.24 | 3.0 | 3.30 |
| 4.5- 6.8 | 3.42-3.58 | 5.0- 6.0 | 3.45-3.55 | 7.0- 9.0 | 4.05-4.15 | 11.0- 17.0 | 3.88-4.08 | 13.0- 17.0 | 3.20-3.40 |
| 8.0- 14.0 | 3.70-4.00 | 10.0- 12.0 | 4.00-4.20 | 9.5- 12.5 | 3.33-3.43 | 15.0- 22.5 | 4.16-4.41 | 7.5- 12.5 | 3.83-4.07 |
| 32.5- 52.5 | 4.60-4.80 | 52.5- 57.5 | 4.60-4.70 | 45.0- 50.0 | 4.62-4.75 | 20.0- 30.0 | 4.38-4.62 | 40.0- 50.0 | 4.38-4.62 |
| 40.0- 70.0 | 4.20-4.40 | 17.5- 22.5 | 4.10-4.20 | 30.0- 45.0 | 4.12-4.38 | 65.0- 85.0 | 4.38-4.62 | 65.0- 80.0 | 4.38-4.62 |
| 127.5-150 | 4.40-4.60 | 145-160 | 4.45-4.55 | 40.0- 65.0 | 4.40-4.60 | 60.0- 85.0 | 4.60-4.80 | 50.0- 90.0 | 4.40-4.60 |

| W-66N12 | | W-68N12 | | W-70N12 | | W-72N12 | | W-74N12 | |
|------------|-----------|------------|-----------|------------|-----------|------------|-----------|------------|-----------|
| h (km) | Vs(km/s) |
| 1.6 | 0.00 | 0.5 | 0.00 | 2.0 | 0.00 | 1.0 | 0.00 | 1.8 | 0.00 |
| 1.5 | 1.10 | 1.5 | 1.10 | 1.0 | 1.20 | 1.5 | 1.00 | 0.8 | 1.10 |
| 0.5 | 1.60 | 0.5 | 1.60 | 4.0 | 2.20 | 4.0 | 1.90 | 1.3 | 2.53 |
| 7.0 | 3.40 | 10.0 | 3.40 | 4.0 | 3.40 | 7.0 | 3.40 | 1.3 | 2.53 |
| 12.5- 17.5 | 3.50-3.70 | 8.0- 12.0 | 3.40-3.60 | 7.5- 12.5 | 3.25-3.55 | 8.0- 14.0 | 3.90-4.00 | 4.0- 7.0 | 3.00-3.20 |
| 5.0- 12.5 | 4.25-4.45 | 4.0- 9.0 | 3.70-3.90 | 20.0- 25.0 | 4.15-4.30 | 7.0- 15.0 | 3.95-4.10 | 8.8- 16.2 | 3.35-3.65 |
| 40.0- 50.0 | 4.38-4.62 | 35.0- 50.0 | 4.38-4.62 | 20.0- 35.0 | 4.62-4.75 | 20.0- 35.0 | 4.38-4.62 | 20.0- 40.0 | 4.40-4.60 |
| 45.0- 70.0 | 4.38-4.62 | 45.0- 70.0 | 4.38-4.62 | 30.0- 50.0 | 4.62-4.75 | 60.0- 80.0 | 4.38-4.62 | 55.0- 80.0 | 4.40-4.60 |
| 50.0- 80.0 | 4.40-4.60 | 50.0- 80.0 | 4.40-4.60 | 75.0-125.0 | 4.40-4.60 | 75.0-100.0 | 4.40-4.60 | 70.0-130.0 | 4.40-4.60 |

| W-76N12 | | W-78N12 | | W-80N12 | | W-82N12 | | W-84N12 | |
|------------|-----------|------------|-----------|------------|-----------|------------|-----------|------------|-----------|
| h (km) | Vs(km/s) |
| 2.8 | 0.00 | 2.4 | 0.00 | 3.0 | 0.00 | 1.5 | 0.00 | 1.6 | 1.10 |
| 0.1 | 0.64 | 0.2 | 2.35 | 0.6 | 1.10 | 1.0 | 0.64 | 2.0 | 2.65 |
| 0.1 | 0.66 | 0.3 | 2.40 | 1.0 | 1.12 | 0.5 | 1.93 | 4.0 | 2.65 |
| 0.1 | 1.96 | 0.1 | 2.60 | 1.5 | 2.00 | 1.0 | 1.93 | 5.1 | 3.50 |
| 6.2- 8.8 | 3.33-3.48 | 9.0- 11.0 | 3.17-3.23 | 5.0- 7.5 | 4.00-4.20 | 5.0- 8.0 | 3.45-3.55 | 5.5- 8.5 | 3.35-3.65 |
| 7.5- 12.5 | 3.30-3.38 | 5.5- 8.5 | 3.38-3.43 | 11.8- 19.2 | 3.70-3.90 | 10.0- 20.0 | 3.80-3.95 | 7.5- 12.5 | 3.95-4.10 |
| 20.0- 30.0 | 4.20-4.40 | 25.0- 35.0 | 4.40-4.60 | 18.0- 36.0 | 4.60-4.80 | 30.0- 50.0 | 4.40-4.60 | 35.0- 55.0 | 4.50-4.70 |
| 27.5- 42.5 | 4.40-4.60 | 20.0- 30.0 | 4.20-4.40 | 85.5-108.0 | 4.40-4.60 | 50.0- 75.0 | 4.20-4.40 | 20.0- 50.0 | 4.10-4.25 |
| 140-160 | 4.40-4.60 | 140-160 | 4.40-4.60 | 75.0-105.0 | 4.40-4.60 | 100-140 | 4.40-4.60 | 130-160 | 4.40-4.60 |

| W-60N14 | | W-62N14 | | W-64N14 | | W-66N14 | | W-68N14 | |
|------------|-----------|------------|-----------|------------|-----------|------------|-----------|------------|-----------|
| h (km) | Vs(km/s) |
| 2.0 | 0.00 | 0.5 | 0.00 | 2.2 | 0.00 | 3.7 | 0.00 | 4.2 | 0.00 |
| 2.0 | 2.05 | 3.0 | 2.60 | 1.5 | 1.20 | 0.5 | 1.20 | 1.5 | 1.20 |
| 4.0 | 2.50 | 8.0 | 3.26 | 2.0 | 1.60 | 0.5 | 1.60 | 1.5 | 1.60 |
| 9.5 | 3.36 | 8.0 | 3.26 | 5.0 | 3.40 | 2.7 | 2.50 | 1.7 | 2.50 |
| 22.0- 26.0 | 3.88-4.03 | 8.0- 11.0 | 4.00-4.20 | 5.0- 7.5 | 3.28-3.53 | 5.0- 10.0 | 3.28-3.53 | 4.0- 8.0 | 3.65-3.95 |
| 25.0- 45.0 | 4.58-4.72 | 5.0- 15.0 | 4.12-4.38 | 5.0- 15.0 | 3.48-3.83 | 7.5- 12.5 | 3.55-3.85 | 8.0- 14.0 | 4.05-4.35 |
| 15.0- 30.0 | 4.35-4.65 | 20.0- 32.5 | 4.12-4.38 | 40.0- 60.0 | 4.38-4.62 | 20.0- 30.0 | 4.38-4.62 | 30.0- 50.0 | 4.38-4.62 |
| 30.0- 45.0 | 4.12-4.38 | 67.5- 90.0 | 4.38-4.62 | 40.0- 65.0 | 4.38-4.62 | 75.0- 90.0 | 4.38-4.62 | 30.0- 45.0 | 4.38-4.62 |
| 50.0- 80.0 | 4.40-4.60 | 50.0- 80.0 | 4.40-4.60 | 85.0-120.0 | 4.38-4.62 | 60.0-100.0 | 4.40-4.60 | 100-120 | 4.40-4.60 |

| W-70N14 | | W-72N14 | | W-74N14 | | W-76N14 | | W-78N14 | |
|------------|-----------|------------|-----------|------------|-----------|------------|-----------|------------|-----------|
| h (km) | Vs(km/s) |
| 2.8 | 0.00 | 3.0 | 0.00 | 3.0 | 0.00 | 1.9 | 0.00 | 2.7 | 0.00 |
| 1.5 | 1.10 | 0.1 | 0.84 | 0.1 | 0.64 | 2.3 | 1.20 | 0.4 | 0.64 |
| 2.0 | 1.60 | 0.5 | 2.80 | 0.1 | 2.30 | 0.3 | 1.80 | 0.6 | 2.50 |
| 7.0 | 3.40 | 0.6 | 2.80 | 0.1 | 2.40 | 0.3 | 2.50 | 0.8 | 2.50 |
| 5.0- 7.0 | 3.35-3.65 | 4.0- 6.0 | 3.60-3.70 | 5.0- 6.5 | 3.50-3.55 | 9.0- 11.0 | 3.60-3.80 | 4.0- 6.0 | 3.50-3.70 |
| 11.0- 17.0 | 4.65-4.80 | 10.5- 13.5 | 3.25-3.35 | 12.5- 15.5 | 3.20-3.30 | 4.0- 8.0 | 3.25-3.35 | 10.0- 12.0 | 3.10-3.30 |
| 10.0- 15.0 | 4.38-4.52 | 5.0- 6.5 | 4.00-4.10 | 17.5- 32.5 | 4.58-4.72 | 10.0- 20.0 | 4.35-4.45 | 14.5- 22.0 | 4.75-4.80 |
| 30.0- 45.0 | 4.60-4.80 | 20.0- 30.0 | 4.60-4.70 | 30.0- 50.0 | 4.40-4.60 | 35.0- 65.0 | 4.40-4.60 | 80.0-100.0 | 4.45-4.55 |
| 100-120 | 4.40-4.60 | 140-160 | 4.40-4.60 | 140-160 | 4.40-4.60 | 140-160 | 4.40-4.60 | 100-140 | 4.43-4.57 |

| W-80N14 | | W-82N14 | | W-84N14 | | W-60N16 | | W-62N16 | |
|------------|-----------|------------|-----------|------------|-----------|------------|-----------|------------|-----------|
| h (km) | Vs(km/s) |
| 2.0 | 0.00 | 0.6 | 0.00 | 1.5 | 1.20 | 4.0 | 0.00 | 2.0 | 0.00 |
| 1.3 | 0.64 | 0.4 | 0.64 | 2.0 | 1.60 | 1.0 | 1.50 | 1.6 | 1.50 |
| 1.0 | 2.61 | 0.6 | 0.64 | 1.0 | 3.40 | 1.8 | 2.20 | 2.0 | 2.26 |
| 1.4 | 2.61 | 0.6 | 1.93 | 1.5 | 3.40 | 1.4 | 2.50 | 10.0 | 3.65 |
| 4.2- 6.8 | 4.03-4.17 | 3.0- 5.0 | 3.15-3.35 | 14.0- 22.0 | 3.95-4.05 | 3.0- 4.0 | 3.65-3.95 | 6.0- 8.0 | 3.55-3.85 |
| 11.5- 14.5 | 3.55-3.65 | 7.5- 12.5 | 3.70-3.90 | 7.0- 11.5 | 3.75-4.05 | 30.0- 34.0 | 3.95-4.15 | 10.0- 17.5 | 4.10-4.30 |
| 17.5- 32.5 | 4.58-4.72 | 10.0- 12.5 | 3.60-3.70 | 40.0- 50.0 | 4.40-4.60 | 20.0- 40.0 | 4.60-4.80 | 40.0- 60.0 | 4.40-4.60 |
| 37.5- 45.0 | 4.43-4.57 | 62.5- 77.5 | 4.40-4.60 | 27.5- 52.5 | 4.20-4.40 | 35.0- 65.0 | 4.20-4.40 | 40.0- 60.0 | 4.40-4.60 |
| 100-140 | 4.20-4.40 | 130-160 | 4.40-4.60 | 100-160 | 4.40-4.60 | 50.0- 80.0 | 4.20-4.40 | 60.0- 90.0 | 4.12-4.38 |

| W-64N16 | | W-66N16 | | W-68N16 | | W-70N16 | | W-72N16 | |
|------------|-----------|------------|-----------|------------|-----------|------------|-----------|------------|-----------|
| h (km) | Vs(km/s) |
| 2.0 | 0.00 | 3.9 | 0.00 | 2.1 | 0.00 | 2.6 | 0.00 | 2.5 | 0.00 |
| 1.5 | 1.20 | 1.5 | 1.20 | 0.2 | 0.64 | 0.4 | 0.62 | 0.6 | 0.64 |
| 0.5 | 1.60 | 0.5 | 1.60 | 0.1 | 2.50 | 0.3 | 0.64 | 0.5 | 1.70 |
| 5.0 | 3.40 | 1.7 | 2.50 | 0.1 | 2.50 | 0.3 | 1.90 | 0.5 | 1.70 |
| 5.0- 9.0 | 3.10-3.30 | 7.5- 12.5 | 3.53-3.78 | 11.0- 19.0 | 3.00-3.20 | 14.0- 16.0 | 3.45-3.55 | 6.0- 8.0 | 3.65-3.75 |
| 5.0- 8.8 | 3.95-4.10 | 5.0- 15.0 | 4.25-4.40 | 8.0- 16.0 | 3.80-4.20 | 5.0- 7.0 | 3.02-3.17 | 8.0- 12.0 | 3.30-3.35 |
| 40.0- 60.0 | 4.38-4.62 | 20.0- 40.0 | 4.38-4.62 | 17.5- 42.5 | 4.60-4.70 | 19.0- 25.0 | 4.65-4.70 | 3.0- 4.0 | 3.80-4.00 |
| 40.0- 65.0 | 4.38-4.62 | 40.0- 65.0 | 4.38-4.62 | 55.0- 70.0 | 4.40-4.60 | 40.0- 50.0 | 4.55-4.65 | 25.0- 30.0 | 4.55-4.65 |
| 50.0- 80.0 | 4.20-4.40 | 35.0-120.0 | 4.40-4.60 | 70.0-130.0 | 4.40-4.60 | 70.0-130.0 | 4.20-4.40 | 140-160 | 4.40-4.60 |

| W-74N16 | | W-76N16 | | W-78N16 | | W-80N16 | | W-82N16 | |
|------------|-----------|------------|-----------|------------|-----------|------------|-----------|------------|-----------|
| h (km) | Vs(km/s) |
| 2.6 | 0.00 | 2.5 | 0.00 | 2.1 | 0.00 | 1.2 | 0.00 | 0.2 | 0.00 |
| 0.2 | 2.40 | 0.8 | 0.64 | 1.0 | 0.64 | 1.3 | 0.84 | 1.0 | 1.10 |
| 0.1 | 2.50 | 0.7 | 3.40 | 2.8 | 2.60 | 1.0 | 2.40 | 0.5 | 1.93 |
| 0.3 | 2.60 | 1.7 | 3.45 | 6.0 | 3.45 | 2.0 | 2.40 | 0.6 | 1.93 |
| 4.5- 5.2 | 3.50-3.70 | 12.5- 15.5 | 3.27-3.33 | 2.5- 3.8 | 2.95-3.15 | 5.0- 8.0 | 3.50-3.70 | 5.0- 7.0 | 3.50-3.70 |
| 10.0- 15.0 | 3.10-3.20 | 4.0- 6.5 | 3.50-3.90 | 8.2- 10.8 | 3.67-3.83 | 8.8- 16.2 | 3.50-3.70 | 17.5- 22.5 | 3.80-4.00 |
| 5.0- 15.0 | 4.10-4.20 | 10.0- 17.5 | 4.20-4.40 | 50.0- 60.0 | 4.60-4.70 | 30.0- 50.0 | 4.50-4.70 | 30.0- 35.0 | 4.40-4.60 |
| 22.5- 47.5 | 4.40-4.60 | 10.0- 25.0 | 4.40-4.60 | 70.0- 80.0 | 4.43-4.57 | 65.0- 90.0 | 4.40-4.60 | 17.5- 32.5 | 4.20-4.40 |
| 140-160 | 4.40-4.60 | 167.5-190 | 4.40-4.60 | 70.0- 80.0 | 4.40-4.60 | 65.0-115.0 | 4.40-4.60 | 140-160 | 4.40-4.60 |

| W-84N16 | | W-86N16 | | W-60N18 | | W-62N18 | | W-64N18 | |
|------------|-----------|------------|-----------|------------|-----------|------------|-----------|------------|-----------|
| h (km) | Vs(km/s) |
| 0.7 | 0.00 | 0.7 | 0.00 | 4.0 | 0.00 | 3.2 | 0.00 | 1.0 | 0.00 |
| 0.5 | 0.72 | 1.1 | 0.64 | 1.0 | 1.10 | 0.7 | 1.19 | 0.6 | 0.64 |
| 0.8 | 1.93 | 4.4 | 3.25 | 0.5 | 1.60 | 0.7 | 1.19 | 0.6 | 0.64 |
| 1.0 | 1.93 | 5.5 | 3.27 | 0.5 | 1.60 | 0.5 | 1.71 | 0.4 | 1.93 |
| 6.0- 10.0 | 3.65-3.85 | 3.5- 5.5 | 3.80-4.00 | 2.0- 6.5 | 3.70-4.00 | 10.0- 18.0 | 3.48-3.83 | 3.5- 6.5 | 3.40-3.60 |
| 7.5- 12.5 | 3.80-4.10 | 10.0- 20.0 | 4.00-4.20 | 27.5- 32.0 | 3.97-4.22 | 10.0- 15.0 | 4.15-4.45 | 15.5- 20.5 | 3.45-3.55 |
| 17.5- 32.5 | 4.35-4.45 | 30.0- 50.0 | 4.40-4.60 | 27.5- 40.0 | 4.38-4.62 | 5.0- 15.0 | 4.00-4.12 | 5.0- 15.0 | 4.40-4.60 |
| 32.5- 47.5 | 4.25-4.35 | 30.0- 50.0 | 4.20-4.40 | 40.0- 80.0 | 4.12-4.38 | 45.0- 75.0 | 4.38-4.62 | 32.5- 57.5 | 4.20-4.40 |
| 190-200 | 4.45-4.55 | 127.5-150 | 4.40-4.60 | 30.0- 52.5 | 4.20-4.40 | 57.5-102.5 | 4.20-4.40 | 130-160 | 4.40-4.60 |

| W-66N18 | | W-68N18 | | W-70N18 | | W-72N18 | | W-74N18 | |
|------------|-----------|------------|-----------|------------|-----------|------------|-----------|------------|-----------|
| h (km) | Vs(km/s) |
| 1.7 | 0.00 | 2.1 | 0.00 | 1.9 | 0.00 | 0.9 | 0.00 | 1.2 | 0.00 |
| 0.6 | 0.64 | 0.3 | 0.64 | 0.2 | 1.10 | 0.6 | 1.10 | 0.3 | 1.20 |
| 0.8 | 1.60 | 0.8 | 1.60 | 0.3 | 1.10 | 0.5 | 1.80 | 0.2 | 2.10 |
| 0.8 | 1.60 | 0.8 | 1.60 | 0.4 | 1.60 | 0.6 | 1.80 | 0.2 | 2.10 |
| 2.5- 3.8 | 3.05-3.15 | 7.0- 11.0 | 3.55-3.65 | 10.0- 14.0 | 3.38-3.53 | 2.0- 3.0 | 2.77-2.92 | 5.8- 8.2 | 3.20-3.30 |
| 19.8- 22.2 | 3.55-3.65 | 5.0- 7.5 | 3.20-3.40 | 10.0- 12.5 | 3.10-3.30 | 17.5- 20.5 | 3.45-3.55 | 13.0- 17.0 | 3.35-3.45 |
| 7.5- 12.5 | 4.60-4.70 | 7.5- 11.2 | 3.20-3.40 | 32.5- 47.5 | 4.35-4.65 | 30.0- 50.0 | 4.40-4.60 | 47.5- 62.5 | 4.45-4.55 |
| 40.0- 50.0 | 4.40-4.60 | 55.0- 65.0 | 4.40-4.60 | 20.0- 35.0 | 4.40-4.60 | 20.0- 40.0 | 4.40-4.60 | 40.0- 70.0 | 4.50-4.70 |
| 140-160 | 4.40-4.60 | 135-150 | 4.40-4.60 | 140-160 | 4.40-4.60 | 155-170 | 4.40-4.60 | 100-160 | 4.40-4.60 |

| W-76N18 | | W-78N18 | | W-80N18 | | W-82N18 | | W-84N18 | |
|------------|-----------|------------|-----------|------------|-----------|------------|-----------|------------|-----------|
| h (km) | Vs(km/s) |
| 1.9 | 0.00 | 1.1 | 0.00 | 2.5 | 0.00 | 3.0 | 0.00 | 2.8 | 0.00 |
| 0.1 | 1.00 | 0.2 | 0.90 | 0.3 | 0.64 | 0.2 | 0.64 | 0.1 | 0.58 |
| 0.1 | 1.10 | 2.0 | 2.71 | 0.3 | 2.54 | 0.2 | 2.50 | 0.2 | 0.58 |
| 0.1 | 2.40 | 2.3 | 2.73 | 0.5 | 2.54 | 0.4 | 2.50 | 0.3 | 2.50 |
| 5.8- 7.2 | 3.00-3.20 | 12.5- 13.5 | 3.25-3.35 | 17.5- 22.5 | 3.67-3.73 | 10.0- 12.0 | 4.05-4.15 | 17.5- 22.0 | 4.00-4.10 |
| 12.5- 15.5 | 3.30-3.50 | 5.0- 12.5 | 4.20-4.40 | 2.0- 4.5 | 3.85-4.15 | 12.0- 16.0 | 3.60-3.80 | 5.5- 10.5 | 3.97-4.22 |
| 45.0- 55.0 | 4.40-4.60 | 25.0- 40.0 | 4.40-4.60 | 12.5- 22.5 | 4.20-4.40 | 20.0- 40.0 | 4.55-4.65 | 60.0- 75.0 | 4.30-4.50 |
| 15.0- 27.5 | 4.60-4.70 | 50.0- 70.0 | 4.40-4.60 | 22.5- 37.5 | 4.40-4.60 | 30.0- 60.0 | 4.20-4.40 | 15.0- 30.0 | 4.20-4.40 |
| 140-160 | 4.40-4.60 | 100-120 | 4.40-4.60 | 175-190 | 4.45-4.55 | 140-160 | 4.40-4.60 | 120-140 | 4.40-4.60 |

| W-86N18 | | W-70N20 | | W-72N20 | | W-74N20 | | W-76N20 | |
|------------|-----------|------------|-----------|------------|-----------|------------|-----------|------------|-----------|
| h (km) | Vs(km/s) |
| 2.8 | 0.00 | 1.4 | 0.00 | 1.7 | 0.00 | 2.2 | 0.00 | 1.8 | 0.00 |
| 0.4 | 0.64 | 0.8 | 0.58 | 0.5 | 0.84 | 0.8 | 1.00 | 0.2 | 1.10 |
| 0.7 | 2.50 | 1.0 | 2.55 | 1.2 | 1.93 | 1.1 | 2.15 | 0.2 | 1.10 |
| 0.9 | 2.50 | 1.8 | 2.55 | 1.2 | 2.10 | 1.2 | 2.15 | 0.5 | 2.60 |
| 3.0- 4.0 | 3.62-3.75 | 5.5- 8.5 | 3.36-3.56 | 22.0- 24.0 | 3.57-3.62 | 15.0- 21.0 | 3.72-3.78 | 14.5- 15.5 | 3.22-3.28 |
| 24.0- 32.0 | 4.10-4.15 | 14.0- 18.0 | 3.45-3.65 | 37.5- 40.0 | 4.35-4.45 | 4.0- 8.0 | 3.25-3.45 | 26.0- 28.0 | 4.22-4.28 |
| 30.0- 45.0 | 4.40-4.60 | 55.0- 65.0 | 4.45-4.55 | 10.0- 15.0 | 4.35-4.45 | 47.5- 62.5 | 4.35-4.45 | 37.0- 43.0 | 4.72-4.78 |
| 37.5- 55.0 | 4.20-4.40 | 30.0- 40.0 | 4.65-4.75 | 35.0- 55.0 | 4.65-4.75 | 35.0- 65.0 | 4.65-4.75 | 72.5- 80.0 | 4.45-4.55 |
| 100-140 | 4.40-4.60 | 145-160 | 4.43-4.57 | 130-160 | 4.40-4.60 | 135-150 | 4.40-4.60 | 80.0-100 | 4.50-4.60 |

| W-78N20 | | W-80N20 | | W-82N20 | | W-84N20 | | W-86N20 | |
|------------|-----------|------------|-----------|------------|-----------|------------|-----------|------------|-----------|
| h (km) | Vs(km/s) |
| 2.8 | 0.00 | 2.5 | 0.00 | 2.9 | 0.00 | 2.7 | 0.00 | 2.8 | 0.00 |
| 0.3 | 1.20 | 0.7 | 1.10 | 0.1 | 0.81 | 0.5 | 0.90 | 0.1 | 1.10 |
| 0.4 | 1.22 | 0.5 | 2.60 | 0.2 | 0.81 | 0.7 | 2.25 | 0.1 | 2.50 |
| 0.6 | 2.50 | 0.8 | 2.60 | 0.4 | 3.40 | 1.0 | 2.50 | 0.2 | 2.80 |
| 3.0- 4.0 | 3.72-3.88 | 16.5- 19.5 | 3.65-3.75 | 22.0- 26.0 | 3.67-3.77 | 10.0- 14.0 | 4.00-4.20 | 18.0- 26.0 | 3.60-3.80 |
| 13.0- 19.0 | 3.35-3.65 | 17.5- 20.0 | 4.28-4.53 | 23.8- 30.0 | 4.30-4.50 | 6.0- 8.5 | 3.25-3.55 | 8.0- 11.5 | 4.05-4.35 |
| 10.0- 15.0 | 4.53-4.67 | 30.0- 50.0 | 4.30-4.50 | 20.0- 30.0 | 4.20-4.40 | 15.0- 30.0 | 4.35-4.45 | 35.0- 50.0 | 4.30-4.50 |
| 22.5- 37.5 | 4.33-4.47 | 25.0- 35.0 | 4.60-4.80 | 30.0- 50.0 | 4.40-4.60 | 85.0-100.0 | 4.40-4.60 | 40.0- 60.0 | 4.35-4.65 |
| 190-200 | 4.50-4.60 | 130-160 | 4.40-4.60 | 127.5-150 | 4.40-4.60 | 100-120 | 4.40-4.60 | 100-140 | 4.40-4.60 |

| W-82N22 | | W-84N22 | | W-86N22 | | W-82N24 | | W-84N24 | |
|------------|-----------|------------|-----------|------------|-----------|------------|-----------|------------|-----------|
| h (km) | Vs(km/s) |
| 0.8 | 0.00 | 1.7 | 0.00 | 1.1 | 0.00 | 0.7 | 0.00 | 2.2 | 0.00 |
| 0.1 | 1.10 | 0.7 | 1.10 | 0.4 | 0.64 | 2.3 | 1.93 | 0.4 | 1.30 |
| 0.2 | 2.30 | 2.0 | 2.40 | 1.0 | 2.20 | 1.0 | 2.40 | 0.5 | 1.70 |
| 0.3 | 2.30 | 2.3 | 2.40 | 1.6 | 2.20 | 1.2 | 2.40 | 0.5 | 1.70 |
| 13.0- 15.0 | 3.15-3.25 | 12.5- 17.5 | 3.60-3.80 | 4.5- 10.5 | 3.25-3.45 | 14.0- 18.0 | 3.55-3.65 | 17.5- 22.5 | 3.55-3.65 |
| 17.0- 19.0 | 3.85-3.95 | 5.0- 7.5 | 3.95-4.25 | 15.0- 25.0 | 3.75-3.95 | 10.0- 22.0 | 4.10-4.30 | 10.0- 20.0 | 4.15-4.30 |
| 7.5- 12.5 | 4.65-4.75 | 35.0- 50.0 | 4.40-4.60 | 25.0- 45.0 | 4.35-4.65 | 22.5- 37.5 | 4.40-4.60 | 15.0- 22.5 | 4.05-4.35 |
| 17.5- 32.5 | 4.25-4.35 | 50.0- 70.0 | 4.40-4.60 | 20.0- 40.0 | 4.40-4.60 | 25.0- 40.0 | 4.60-4.70 | 32.5- 57.5 | 4.60-4.70 |
| 140-160 | 4.45-4.55 | 70.0-130 | 4.40-4.60 | 130-160 | 4.40-4.60 | 140-160 | 4.40-4.60 | 130-160 | 4.40-4.60 |

| W-82N26 | | W-84N26 | | W-76N8 | | W-80N8 | | W-82N8 | |
|------------|-----------|------------|-----------|------------|-----------|------------|-----------|------------|-----------|
| h (km) | Vs(km/s) |
| 0.1 | 0.00 | 0.3 | 0.00 | 0.5 | 1.20 | 0.1 | 0.00 | 0.4 | 0.00 |
| 0.5 | 1.70 | 1.6 | 1.20 | 0.4 | 2.20 | 0.3 | 1.00 | 0.1 | 0.70 |
| 1.3 | 2.50 | 0.6 | 2.50 | 1.3 | 2.23 | 3.0 | 3.00 | 2.0 | 2.60 |
| 1.4 | 2.55 | 0.9 | 2.55 | 1.4 | 2.26 | 3.0 | 3.10 | 3.8 | 2.60 |
| 16.2- 18.8 | 3.35-3.45 | 19.0- 21.0 | 3.65-3.75 | 11.2- 13.8 | 3.10-3.20 | 8.5- 11.5 | 3.05-3.15 | 8.5- 11.5 | 3.20-3.30 |
| 5.0- 8.8 | 3.90-4.10 | 6.5- 10.5 | 3.90-4.10 | 20.0- 26.0 | 4.03-4.28 | 5.0- 7.5 | 4.18-4.40 | 7.5- 12.5 | 4.05-4.35 |
| 17.5- 32.5 | 4.20-4.40 | 15.0- 25.0 | 4.18-4.32 | 25.0- 35.0 | 4.20-4.40 | 40.0- 50.0 | 4.40-4.60 | 30.0- 50.0 | 4.60-4.70 |
| 30.0- 60.0 | 4.60-4.70 | 42.5- 50.0 | 4.65-4.70 | 20.0- 30.0 | 4.60-4.70 | 10.0- 25.0 | 4.10-4.20 | 22.5- 47.5 | 4.20-4.40 |
| 140-160 | 4.40-4.60 | 140-160 | 4.40-4.60 | 140-160 | 4.40-4.60 | 130-160 | 4.40-4.60 | 110-140 | 4.40-4.60 |

References

- Bassin, C., Laske, G. and Masters, G. (2000), "The Current Limits of Resolution for Surface Wave Tomography in North America", EOS Trans. AGU, 81, F897.
- Biswas, N.N. and Knopoff, I. (1974), The structure of the upper mantle under the U.S. from the dispersion of Rayleigh waves, Geophys. J. R. Astr. Soc. 36, 515–539.
- Boyadzhiev, G., Brandmayr, E., Pinat, T. and Panza, G.F., (2008) Optimization for nonlinear inverse problem. Rendiconti Lincei: Scienze Fisiche e Naturali, 19, 17-43.
- Chulick, G. S. and Mooney, W. D. (2002), "Seismic Structure of the Crust and Uppermost Mantle of North America and Adjacent Oceanic Basins: A Synthesis", Bull. Seism. Soc. Am., 92(6), 2478-2492.
- Dengo, G. and Case, J.E. (1990). "The Geology of North America. Volume H. The Caribbean Region", The Geological Society of America, Boulder, U.S.A.
- Ditmar, P.G. and Yanovskaya, T.B. (1987), A generalization of the Backus-Gilbert method for estimation of lateral variations of surface wave velocity, Izv. Akad. Nauk SSSR, Fizika Zemli (6), 30–60.
- Doglioni C., Gueguen, E., Harabaglia P. & Mongelli F. (1999): On the origin of W-directed subduction zones and applications to the western Mediterranean. Geol. Soc. Sp. Publ., 156, 541-561.
- Doglioni C., Carminati E., Cuffaro M. and Scrocca D. (2007): Subduction kinematics and dynamic constraints. Earth Science Reviews, 83, 125-175, doi:10.1016/j.earscirev.2007.04.001.
- Doglioni C., Tonarini S. and Innocenti F., (2009), Mantle wedge asymmetries and geochemical signatures along W- and E-NE-directed subduction zones. Lithos, doi:10.1016/j.lithos.2009.01.012
- Du, Z.J., Michelini, A., and Panza, G.F. (1998). "EurID: a regionalised 3-D seismological model of Europe". Phys. Earth Planet. Inter., 105, 31-62.
- Fowler, C.M.R., The Solid Earth. An Introduction to Global Geophysics (Cambridge Univ. Press 1995).
- González, O.; Alvarez, L.; Guidarelli, M.; Panza, G.F. (2007): Crust and Upper Mantle Structure in the Caribbean Region by Group Velocity Tomography and Regionalization. Pure and Applied Geophysics, v. 164, pp. 1985–2007.
- Grant, F.S. and West G.F., Interpretation Theory in Applied Geophysics (McGraw-Hill Inc., New York, U.S.A, 1965).
- Growdon, M. A., Pavlis, G.L. Niu, F., Vernon, F.L. and Rendon, H. (2009) Constraints on the mantle flow at the Caribbean-South American plate boundary inferred from shear wave splitting, J. Geophys. Res. 114, B02303, doi:10.1029/2008JB005887.
- Iturralde, M. and Lidiak, E. (2000). Annual Reports of the project IGCP 433 "Caribbean Plate Tectonics, Origin and Evolution of the Region" (<http://www.ig.utexas.edu/CaribPlate/CaribPlate.html>)
- Laske, G. and Masters, G. (1997), A global digital map of sediment thickness, EOS Trans. AGU 78, F483.

- Levshin, A.L., Pisarenko, V.F., and Pogrebinsky, G.A. (1972), On a frequency-time analysis of oscillations, *Ann. Geophys.* 28(2), 211–218.
- Levshin, A.L., Radnikova, L.I., and Berger, J. (1992), Peculiarities of surface wave propagation across Central Eurasia, *Bull. Seismol. Soc. Am.* 82, 2464–2493.
- Ligorría J.P. and Molina, E. (1997), “Crustal Velocity Structure of Southern Guatemala using Refracted and Sp Converted Waves”, *Geofisica Intern.*, 36(1).
- Magnani, M.B., Zelt, C.A., Levander, A. and Schmitz, M. (2009), Crustal structure of the South-American plate boundary at 67° from controlled seismic data, *J. Geophys. Res.* 114, B02312, doi:10.1029/2008JB005817.
- Mann, P., Prentice, C.S. Burr, G. Pena, L.R., Taylor , F.W. (1998): Tectonic evolution geomorphology and paleoseismology of the Septentrional fault system, Dominican Republic, In: Active strike-slip and Collisional Tectonics of the Northern Caribbean Plate Boundary Zone. Geological Society of America Special Paper 326, Geological Society of America, Boulder, Colorado, pp. 63-123.
- Mann, P., E. Calais, J.-C. Ruegg, C. DeMets, P. E. Jansma, and G. S. Mattioli (2002): Oblique collision in the northeastern Caribbean from GPS measurements and geological observations, *Tectonics*, 21(6), 1057, doi:10.1029/2001TC00134.
- Miller, M.S., Levander, A., Niu,F. and Li, A. (2009), Upper mantle structure beneath the Caribbean-South American plate boundary from surface wave tomography, *J. Geophys. Res.* 114, B01312, doi:10.1029/2007JB005507.
- Montagner, J.P. and Kennet, B.L.N. (1996), How to reconcile body-wave and normal-mode referente Earth models, *Geophys. J. Int.* 125, 229–248.
- Mooney, W.D., Laske, G., and Masters, T.G. (1998), CRUST 5.1: A global crustal model at 5°x5°, *J. Geophys. Res.* 103(B1), 727–747.
- Moreno, B., Grandison, M., and Atakan, K. (2002), Crustal velocity model along the Southern Cuban margin: Implications for the tectonic regime at an active plate boundary, *Geophys. J. Int.* 151, 632–645.
- Panza, G.F., The Resolving power of seismic surface waves with respect to crust and upper mantle structural models, In The Solution of the Inverse Problem in Geophysical Interpretation (Cassinis, R. ed.) pp. 39–77.(Plenum Publ. Corp. 1981)
- Panza G., Doglioni C. and Levshin A. (2010): Asymmetric ocean basins. *Geology*, 38, 1, p. 59-62, doi: 10.1130/G30570.1.
- Pindell, J. and Kennan, L. (2001). “Kinematic Evolution of the Gulf of Mexico and Caribbean”. In: GCSSEPM Research Conference (Richard Fillon, ed.), Houston, U.S.A.
- Pindell, J. and Kennan, L.,(2009). Tectonic evolution of the Gulf of Mexico, Caribbean and northern Sotuh America in the mantle reference frame: an update. In press in: The geology and evolution of the region between North and South America, Geological Society of London, Special Publication.
- Shapiro, N.M. y Ritzwoller, M.H. (2002). Monte-Carlo inversion for a global shear velocity model of the crust and upper mantle. *Geophysics Journal International*. 151:88105.
- Smith, W.H.F. and Sandwell, D.T. (1997). Global sea floor topography from satellite altimetry and ship depth soundings, *Sci Magaz* 277, issue 5334.

- Ten Brink, Uri S., Coleman, Dwight F., and Dillon, William P. (2001). Asymmetric seafloor spreading, crustal thickness variations and transitional crust in Cayman trough from gravity, Paper No. 63-0 GSA Annual Meeting, November 5-8, 2001. Boston, Massachusetts.
- Ten Brink, U.S., Coleman, D.F., and Dillon, W.P. (2002). The nature of the crust under Cayman Trough from gravity. *Marine and Petroleum Geology*, v. 19, pp. 971-987.
- Tenreyro, R., López, J. G., Echevarría, G., Alvarez, J., Sánchez, J. R. (1994). Geologic Evolution and Structural Geology of Cuba. Abstracts AAPG Annual Meeting, June 12- 15. Denver. Colorado.
- Urban, L., Cichowicz, A. and Vaccari, F. (1993). "Computation of Analytical Partial Derivatives of Phase and Group Velocities of Rayleigh Waves Respect to Structural Parameters". *Studia Geoph. Et Geod.*, 36, 14-36.
- Valyus, V.P. (1968), Determining seismic profiles from a set of observations (in Russian), *Vychislitel'naya Seismologiya* 4, 3–14. English translation: Computational Seismology (V.I. Keylis-Borok, ed.) pp. 114–118, (Consultants Bureau, 1972).
- Van der Hilst, R. D. (1990): "Tomography with P, PP and pP Delay-time Data and the Three-dimensional Mantle Structure below the Caribbean Region", Ph.D. Thesis, University of Utrecht, Holand.
- Vdovin, O., Rial, J.A., Levshin, A.L. and Ritzwoller, M. H. (1999). "Group-velocity Tomography of South America and the Surrounding Oceans". *Geophys. J. Int.*, 136, 324-340.
- Wu, F.T. and Levshin, A. (1994), Surface-wave group velocity tomography of east Asia, *Phys. Earth Planet Int.* 84, 59–77.
- Yanovskaya, T.B. and Ditmar, P.G. (1990), Smoothness criteria in surface wave tomography, *Geophys. J. Int.* 102, 63–72.
- Yanovskaya, T.B. (1997), Resolution estimation in the problems of seismic ray tomography, *Izvestiya, Physics of the Solid Earth* 33(9), 762–765.

Table 1. Seismic stations used for this study. SSSN – Cuban National Seismological Survey, GSN – Global Seismic Network, FUN – Venezuelan Foundation of Seismological Research, IU - Global Seismograph Network (GSN - IRIS/USGS), CU - Caribbean Network (USGS), G – GEOSCOPE, INET – INETER, XT - South Eastern Caribbean Passive Experiment.

| Código | Región | Latitud (N) | Longitud (W) | Altura (m) | Red |
|--------|--------------------------------------|-------------|--------------|------------|------|
| RCCC | Rio Carpintero | 19.999 | 75.696 | 100 | SSSN |
| CCCC | Cascorro | 21.200 | 77.766 | 150 | SSSN |
| LMGC | Las Mercedes | 20.064 | 77.005 | 220 | SSSN |
| MOAC | Moa | 20.660 | 74.960 | 120 | SSSN |
| MASC | Maisi | 20.175 | 74.231 | 320 | SSSN |
| MGV | Manicaragua | 22.110 | 79.980 | 300 | SSSN |
| SOR | Soroa | 22.784 | 83.008 | 206 | SSSN |
| DWPF | Disney Wilderness Preserve | 28.110 | 81.433 | 142 | GSN |
| HKT | Hockley | 29.950 | 95.833 | 415 | GSN |
| SDV | Santo Domingo (Vzla) | 8.886 | 70.633 | 1580 | GSN |
| TEIG | Tepich | 20.226 | 88.276 | 69 | GSN |
| SJG | San Juan | 18.112 | 66.150 | 457 | GSN |
| JTS | Juntas de Abangares | 10.291 | 84.952 | 340 | GSN |
| FUNV | El Llanito, Venezuela | 10.470 | 66.810 | 875 | FUN |
| CUPV | Cupira, Venezuela | 10.057 | 65.788 | 668 | FUN |
| MERV | Las Mercedes, Venezuela | 9.251 | 66.297 | 156 | FUN |
| CRUV | Carúpano, Venezuela | 10.675 | 63.236 | 20 | FUN |
| MONV | Montecano, Venezuela | 11.955 | 69.971 | 170 | FUN |
| ITEV | Isla los Testigos, Venezuela | 11.355 | 63.132 | 13 | FUN |
| IBAW | Isla La Blanquilla, Venezuela | 11.823 | 64.577 | 100 | FUN |
| ORIV | Oritupano, Venezuela | 9.070 | 63.409 | 123 | FUN |
| TURV | Turiamo, Venezuela | 10.450 | 67.840 | 58 | FUN |
| ORCV | Isla La Orchila | 11.812 | 66.194 | 22 | FUN |
| MPGF | Montagnes des Peres, Guyana F. | 5.110 | 52.644 | 147 | G |
| ANWB | Willy Bob, Antigua y Barbuda | 17.669 | 61.786 | 39 | CU |
| BBGH | Gun Hill, Barbados | 13.143 | 59.559 | 180 | CU |
| BCIP | Isla Barro Colorado, Panama | 9.166 | 79.837 | 61 | CU |
| BOA | Boaco, Nicaragua | 12.482 | 85.718 | 550 | INET |
| FDF | Fort de France | 14.733 | 61.150 | 510 | G |
| GRGR | Grenville, Grenada | 12.132 | 61.654 | 195 | CU |
| GRTK | Grand Turk, Turks and Caicos Islands | 21.511 | 71.133 | 12 | CU |
| GTBY | Guantanamo Bay, Cuba | 19.927 | 75.111 | 79 | CU |
| HDC | Heredia, Costa Rica | 10.000 | 84.112 | 1186 | G |
| MTDJ | Mount Denham, Jamaica | 18.226 | 77.534 | 925 | CU |
| OTAV | Otavalo, Ecuador | 0.2398 | 78.451 | 3510 | IU |
| SAML | Samuel, Brazil | 8.949 | 63.183 | 120 | IU |
| SDDR | Presa Sabenta, República Dominicana | 18.982 | 71.288 | 589 | CU |
| TGUH | Tegucigalpa, Honduras | 14.057 | 87.273 | 0 | CU |
| BBSR | St George's Bermuda | 32.371 | 64.696 | 30 | IU |

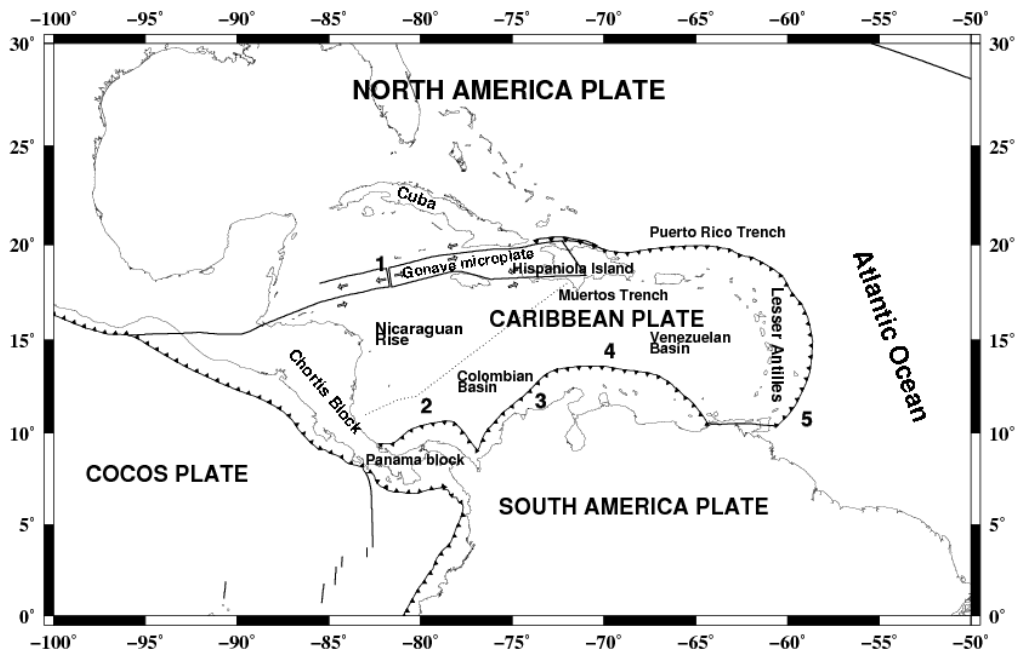


Figure 1. Schematic map of Caribbean region (modified from Gonzalez et al., 2007). (1. Mid Cayman Spreading Center in the Cayman trough, 2. Northern Panama deformed belt, 3. South America deformed belt, 4. South Caribbean fold belt and 5. Barbados Prism).

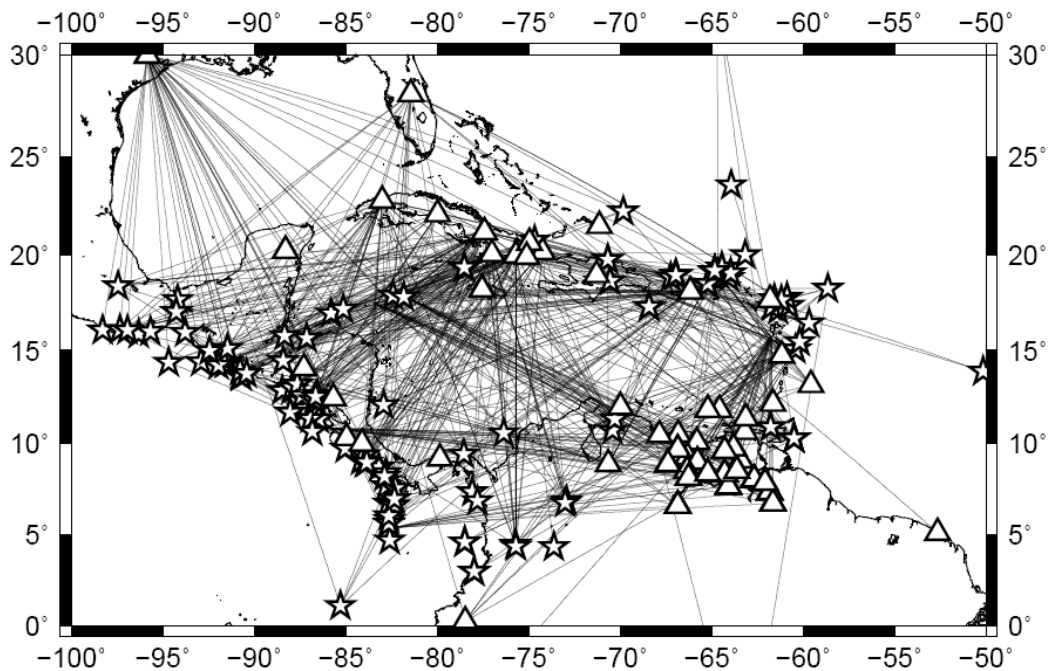


Figure 2. Epicenters (stars), stations (triangles) and seismic paths selected for surface-wave tomography.

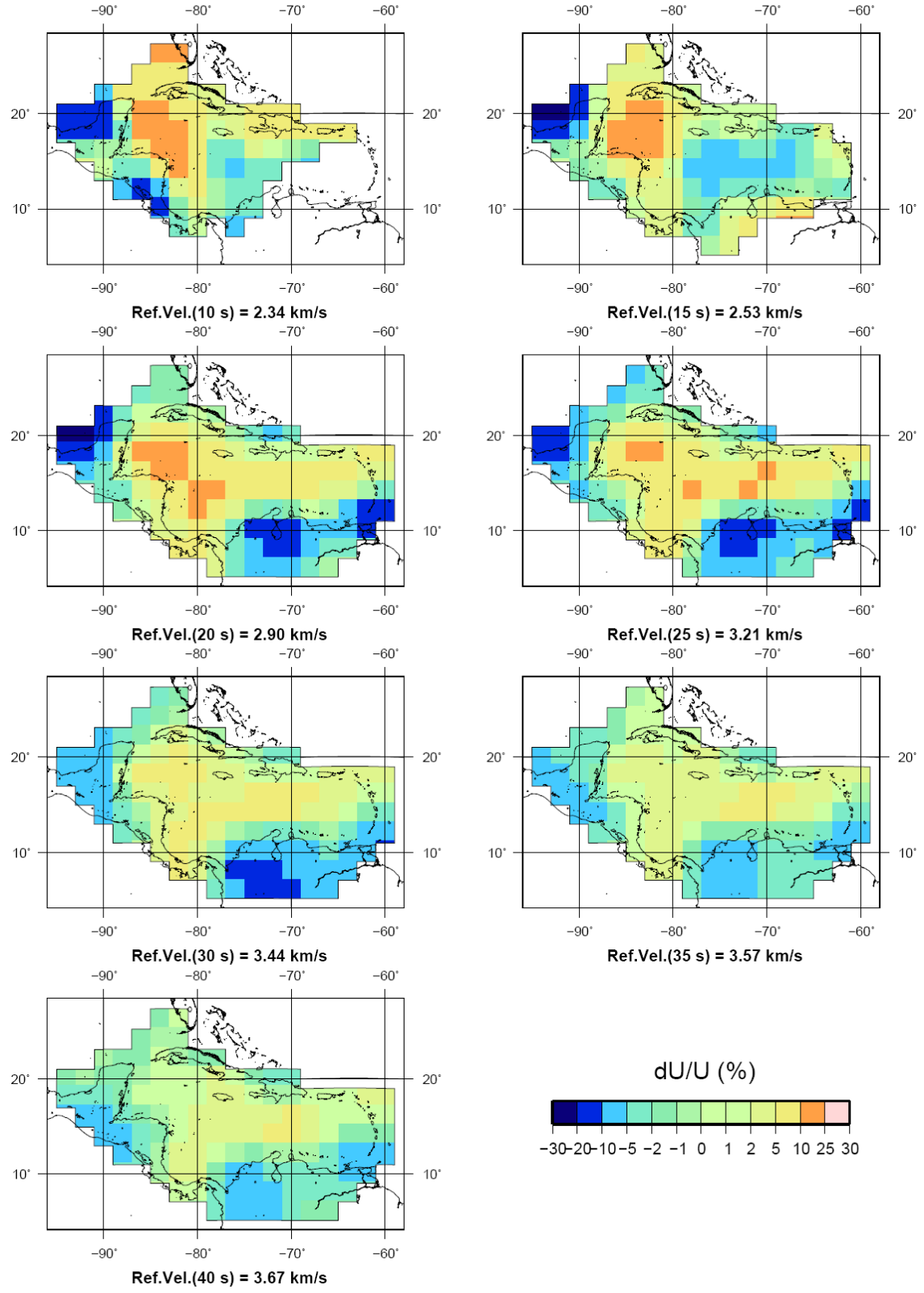


Figure 3. Rayleigh waves group velocity tomography at different periods (10 s – 40 s) shown as percent deviation from the average reference velocity at each period (Ref. Vel.).

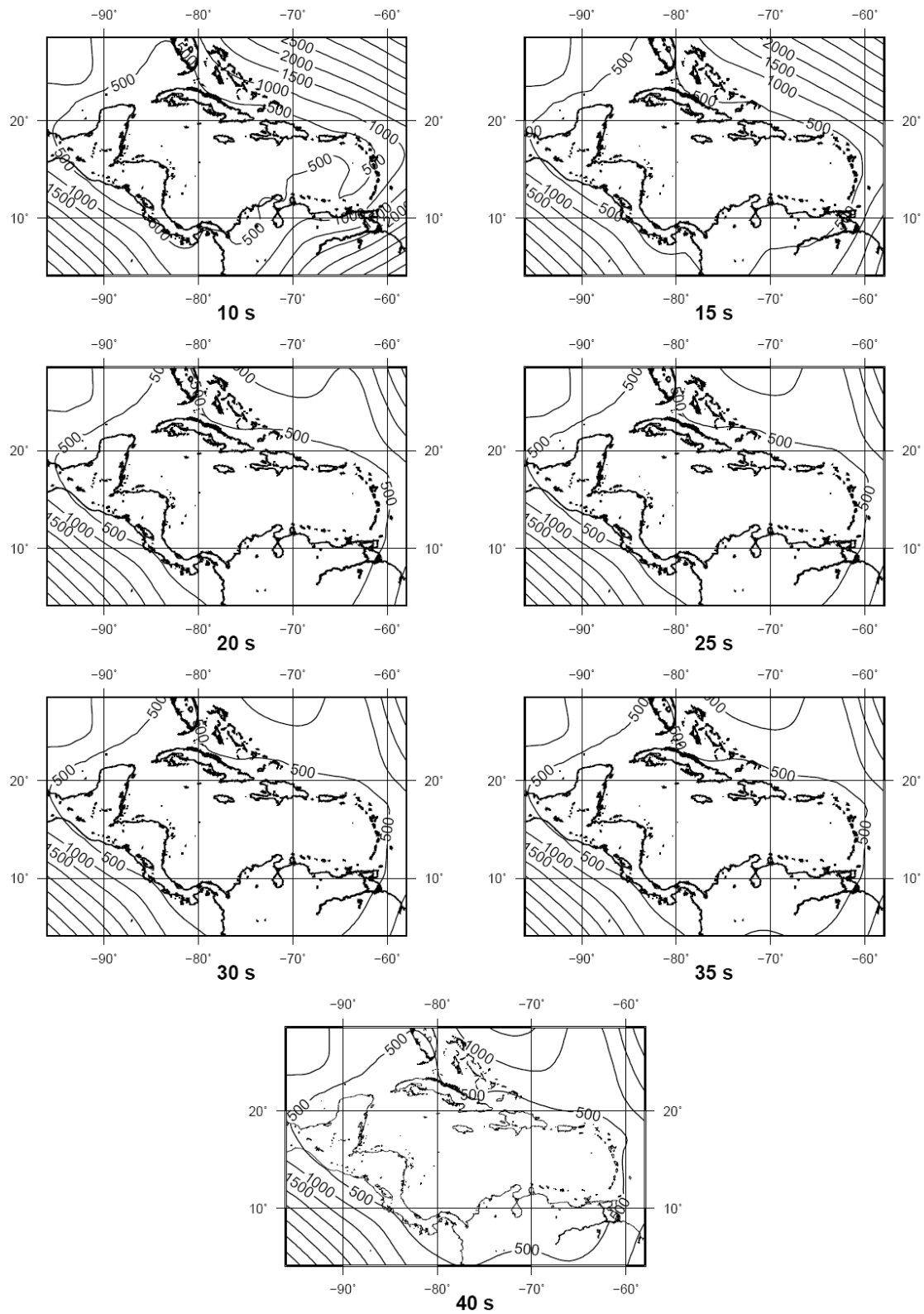


Figure 4. Maps of (a), the horizontal resolution (km) at different periods (10 s – 40 s).

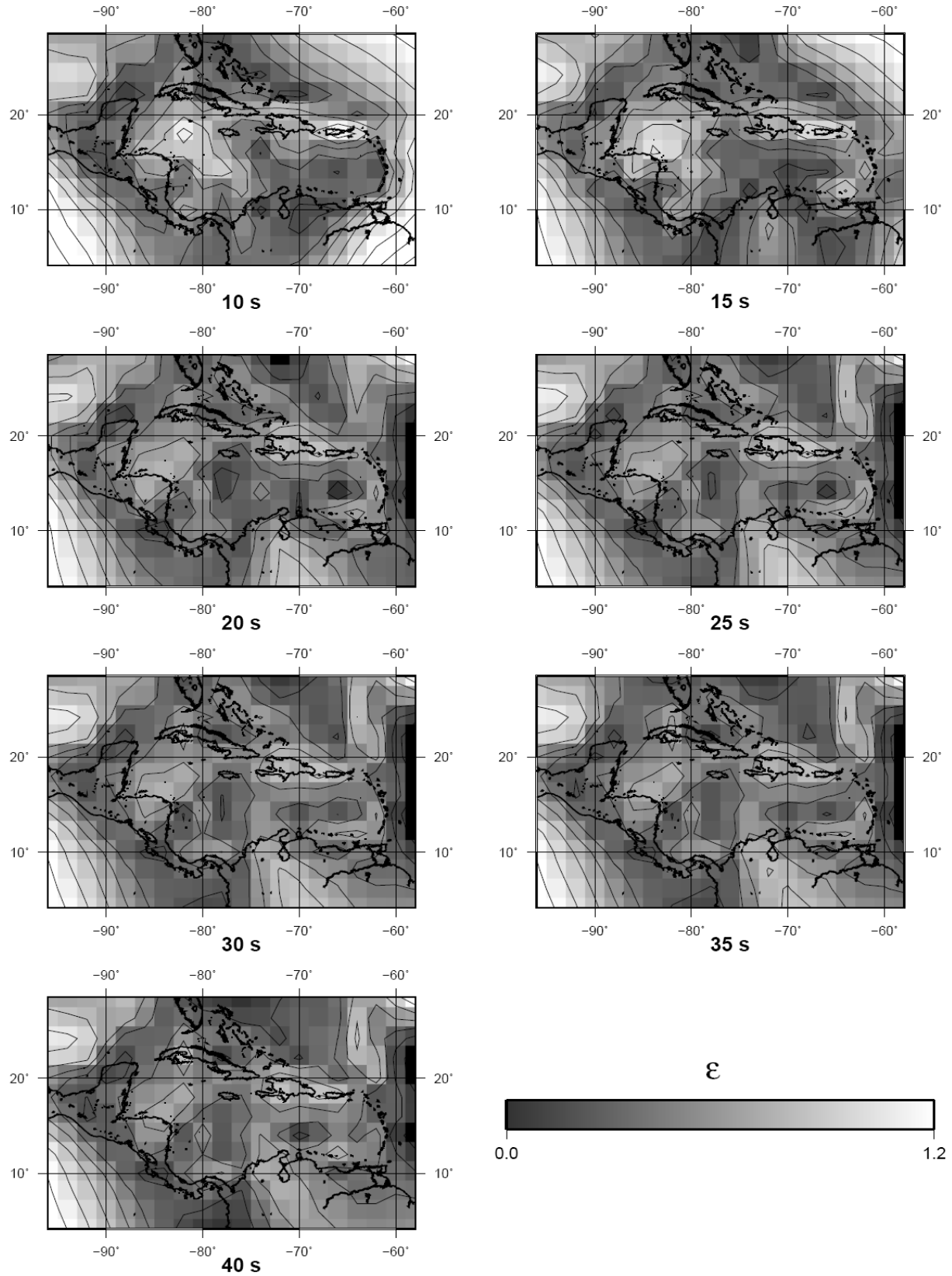


Figure 5. Maps of the azimuthal resolution, $\epsilon = 2b/a$, at different periods (10 s – 40 s). Small values of ϵ (≤ 0.5) indicate that the obtained solution is locally smoothed over an area of the same size in all directions, large values ($\epsilon \geq 1$) indicate that a preferred orientation of the paths exists.

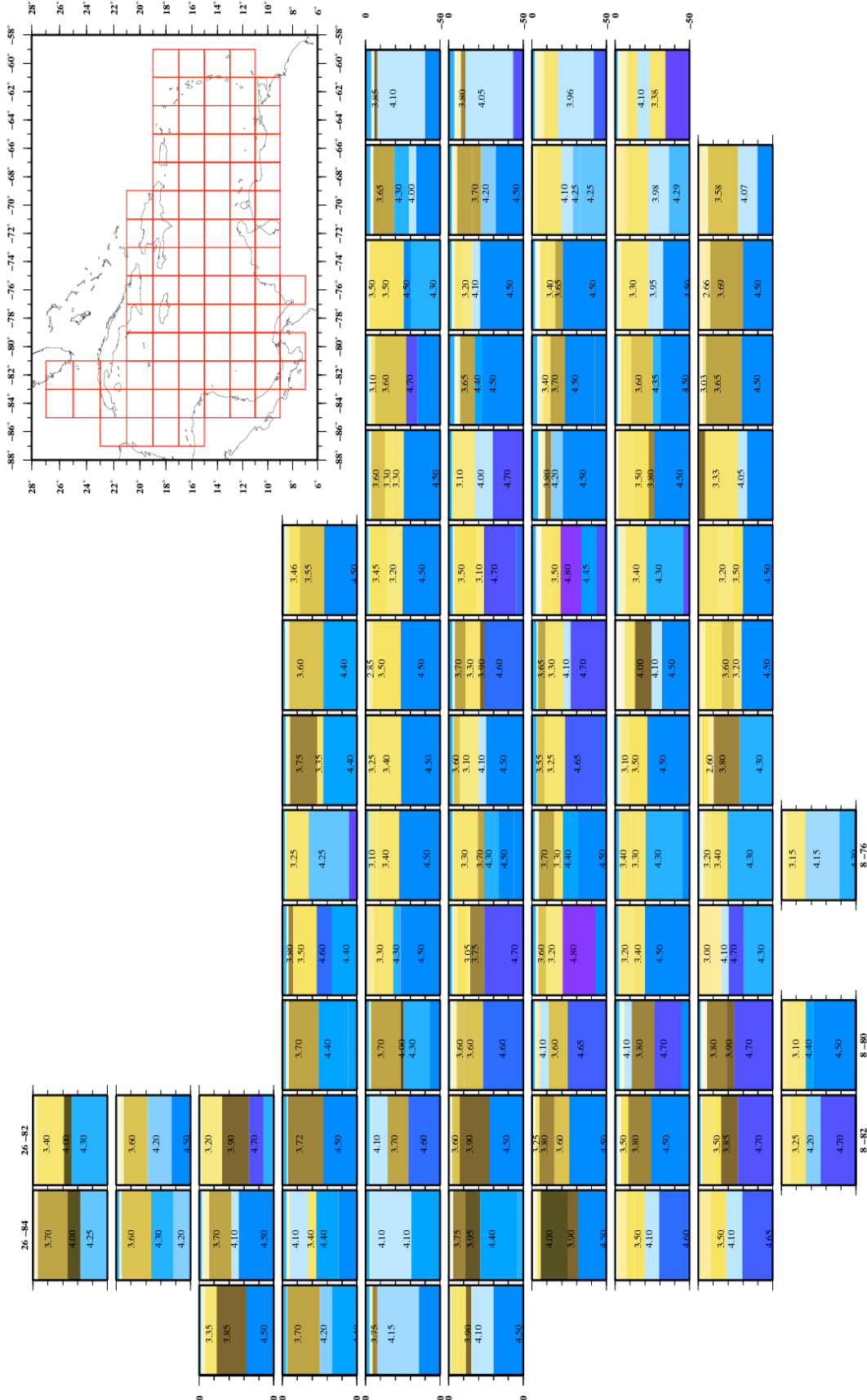


Figure 6. Vs vs. depth models up to 50 km. The numbers correspond to the Vs velocities of the selected solution by LSO and their ranges of variability are in Appendix 2.

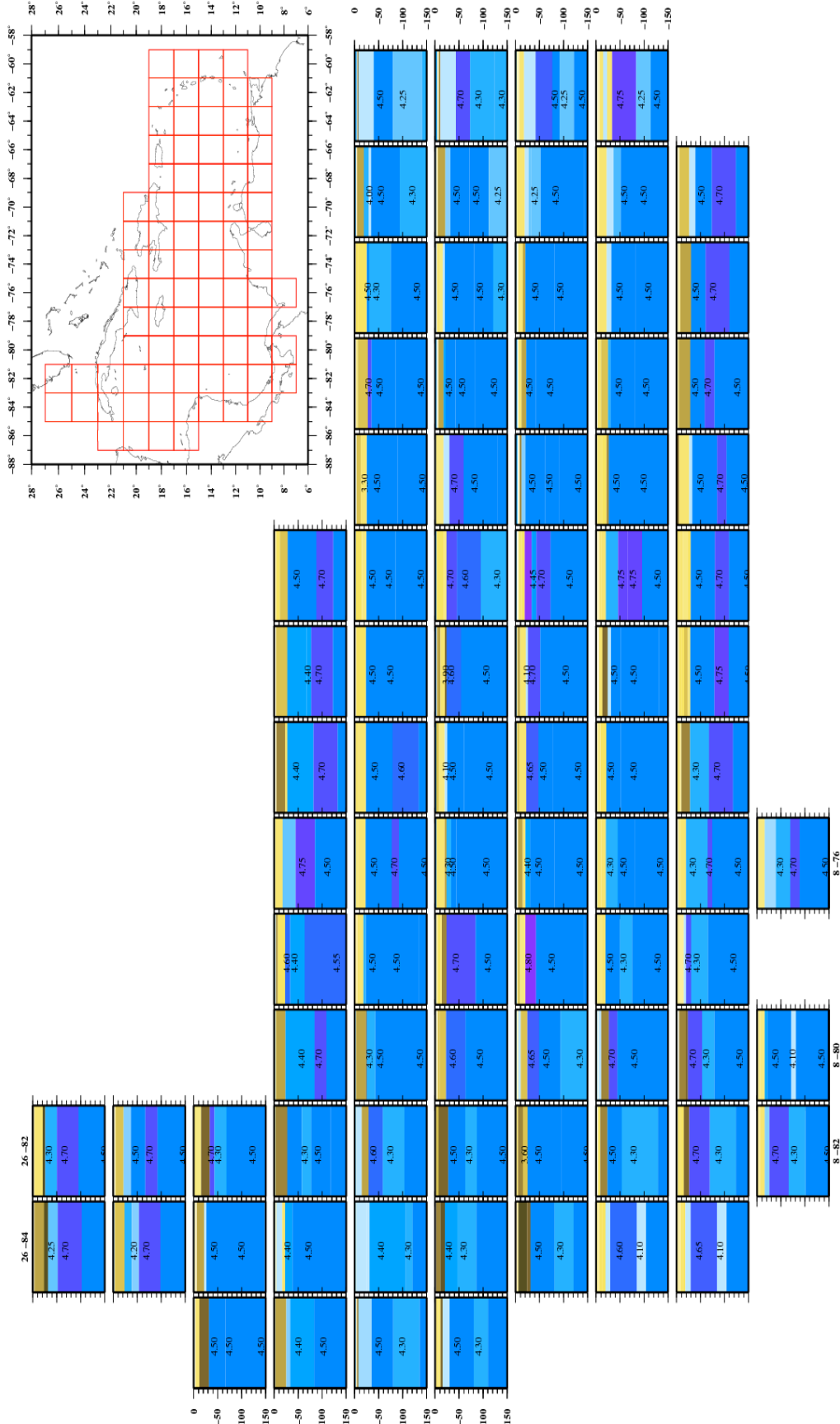


Figure 7. Vs vs. depth models up to 150 km.

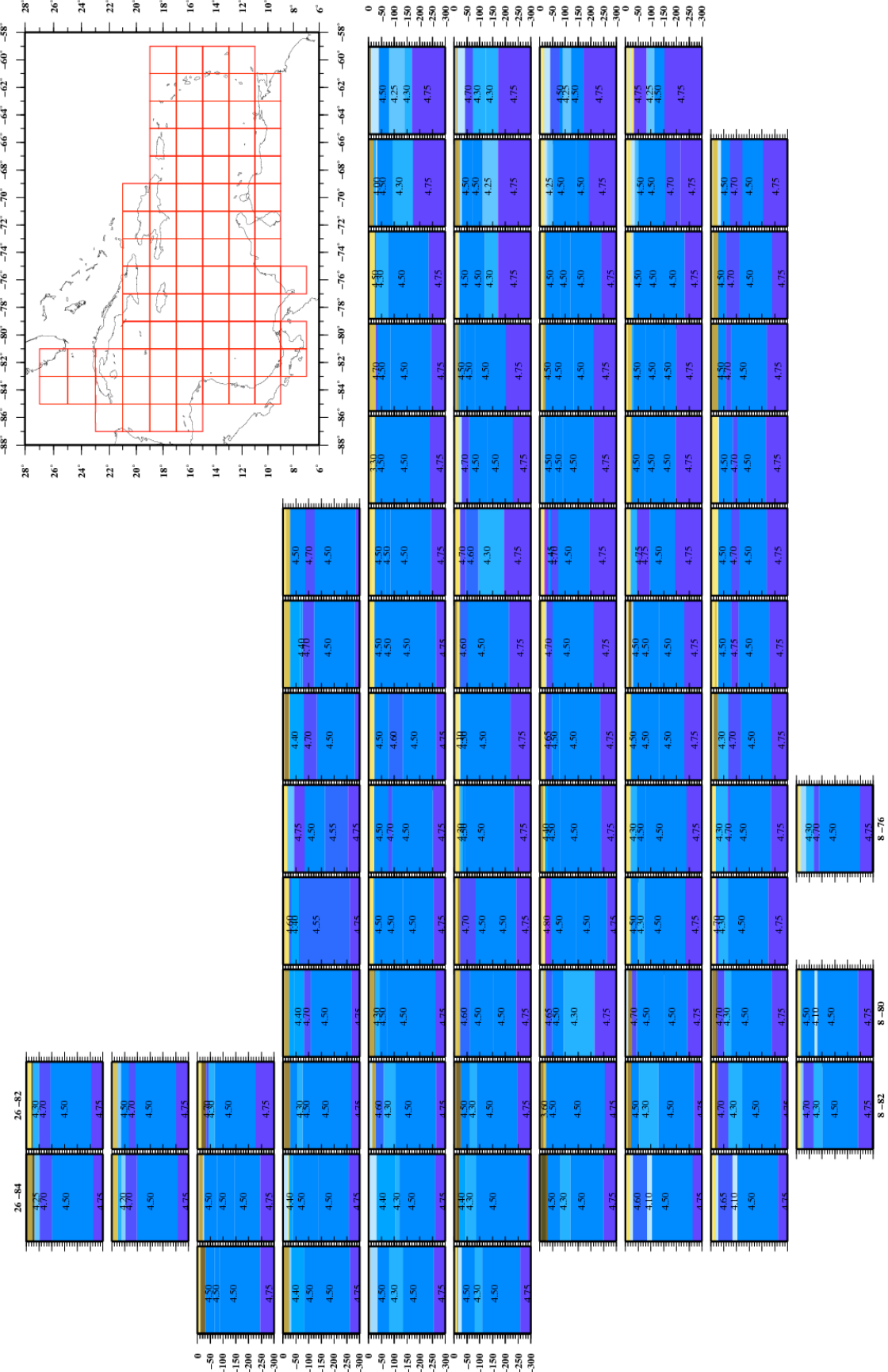


Figure 8. Vs vs. depth models up to 300 km.

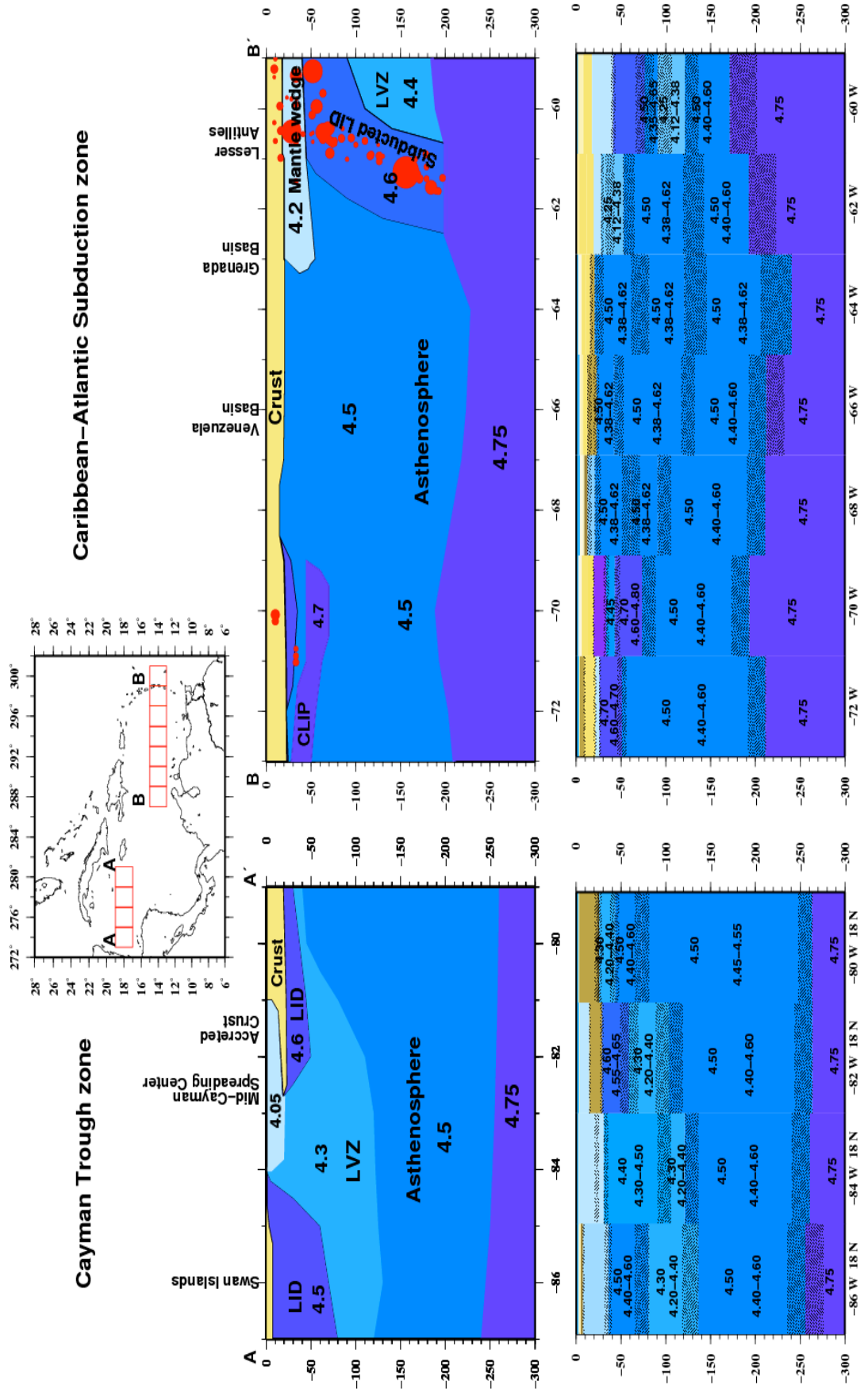


Figure 9. Profiles Vs vs. depth along the Cayman trough and the Caribbean subduction zone and the corresponding schematic interpretative cartoons. (CLIP, Caribbean Large Igneous Province; LVZ, low velocity zone). In the interpretation some representative values are given that fall within the uncertainty range